

RWS lander deployment 2010

Report on environmental monitoring off the coast of
Egmond in the year 2010.



Rob Witbaard, Gerard Duineveld, Magda Bergman.

NIOZ, Postbus 59, 1790AB Den Burg Texel

Commissioned by:
Foundation La Mer
Postbus 474
2800 AL Gouda

Colophon

Report number:	NIOZ report 2011-project 2694
Published by:	Foundation La Mer
Referentienummer	LM-10092/10093
Date:	November 2011
Authors:	R. Witbaard, G. Duineveld, M. Bergman
Title:	Report on continuous environmental monitoring off the coast of Egmond in the year 2010.
Project name:	RWS short Deploy
Commissioned by:	Foundation La Mer, Postbus 474 2800 AL Gouda
Programme:	Monitoring and Evaluation Programme Sand mining RWS LaMER, part B5 of the evaluation programme Sand mining (Ellerbroek e.a. 2008). Monitoring and Evaluation Programme Sand mining Sand engine
Partners	Foundation La Mer Rijkswaterstaat Project realisation Sand engine

Supervised by:	Marcel Rozemeijer (RWS-WD) Saa H. Kabuta (RWS-WD) John de Ronde (Deltares) Johan de Kok (Deltares) Rik Duijts (RWS-DNZ) Evelien van Eijsbergen (RWS-WD)
Executed by:	NIOZ Netherlands Institute for Sea Research Landsdiep 4, 1797 SZ, Den Hoorn (Texel)
Availability:	This report is available on the Rijkswaterstaat website as a PDF file from http://www.rijksoverheid.nl/documenten-en-publicaties/rapporten).
Tasks:	
Analyses & Reporting	Rob Witbaard, Gerard Duineveld, Magda Bergman.
Lab work organization	Rob Witbaard, Magda Bergman. Logistics – Rob Witbaard, Magda Bergman Lab Work – Joost van der Hoek, Evaline van Weerlee
Field work	Crew Navicula, Rob Witbaard, Gerard Duineveld, Magda Bergman, Evaline van Weerlee, Carola van der Hout, Joost van der Hoek, Maarten Mulder.
Project management	Rob Witbaard, Magda Bergman
To be quoted as:	Witbaard R, GCA Duineveld & M. Bergman (2011). Environmental monitoring off the coast of Egmond in 2010. NIOZ Report 2011-project 2624

INTRODUCTION	5
METHODS	9
Lander Deployments	9
Valvometry	13
Additional sampling	13
Lab procedures	15
Ash Free dry weights.....	15
RESULTS.....	16
<i>Ensis directus</i>	16
Weight and condition	22
Environmental Data.	23
Temperature and Salinity.....	23
Currents.	25
Suspended matter.	26
Valvometry	33
Spring.....	33
Autumn.....	37
Harbour experiment.....	41
DISCUSSION & SYNTHESSES.....	46
CONCLUSIONS.....	50
REFERENCES	52

INTRODUCTION

Continuous efforts to protect the Dutch coastline from erosion as well as large infra structural works such as Maasvlakte II or the Sand engine require large amounts of sand to be annually supplied onto the coastline (year 2010: > 12 million ton). Since 1997 beach nourishment is alternated with underwater nourishment at the shoreface. In the meantime a large portion of coastal zone has been designated as an area of conservation in the framework of inter- and national agreements (NATURA 2000, Natuurbeschermingswet), because of its ecological value for birds and fish. Especially the abundant bivalves form a basic food source of overwintering birds. Over the past 15 years, a doubling has taken place in the total standing stock of bivalves in the Dutch coastal zone (Figure 1). While in the 1990's, *Spisula subtruncata* was the most abundant species occurring in dense aggregations, nowadays the invasive American razor shell, *Ensis directus*, dominates the biomass. (Goudswaard et al, 2011) The presently known standing stock of *E. directus* is substantially higher than previously reported estimates of bivalve biomass. Because *E. directus* rapidly retracts itself deep in the sediment, accurate density estimates are difficult. Moreover a significant number of *Ensis directus* live in the shallow shoreface (Figure 2) which is difficult to access and sample. *Ensis* density, therefore, is likely even higher (Goudswaard et al, 2008; Goudswaard et al, 2011).

Sand used for shoreface deposition is extracted from off shore locations. In the process of extraction, mud is released. Percentages mud in sediment off the coast vary between 0 and ~3.5%. Because of massive bulk of sand which is extracted, the released amount of mud may be significant on a local scale. Tides transport the suspended material resulting in far field effects i.e. increased turbidity with a reduced primary production away from the extraction areas. As such the reduced primary production as well as the increased amounts of SPM may have an impact on growth and production of filterfeeding bivalves in the coastal zone. Also the shore face deposition and beach nourishments lead to local effects in the near coastal zone.

To study some of the side effects of sand mining and shoreface deposition, two important research questions of the Monitoring programme RWS LaMER were defined:

- (1) What are the effects of the reduced food conditions on the growth of *E. directus*
- (2) When does food limitation occur as a result of these changed conditions?

Many filter-feeding invertebrates (bivalves and polychaetes) show a depressed filtration activity and growth rate in the presence of large concentrations of suspended mud (Wilber and Clarke 2001, Archambault et al 2006). The bivalve species inhabiting the Dutch coastal zone (e.g. *Ensis*, *Macoma*, *Tellina*) have to cope with natural high concentrations of mud. Longshore SPM transport in a narrow strip along the Dutch coast (RIKZ atlas) is estimated to be in the order of 10 to 20 million tons per year (Van Alphen, 1990; De Kok, 2004) but this is most likely an underestimate. Nevertheless, laboratory experiments showed that *Ensis directus* show depressed clearance rates under high mud concentrations (Witbaard & Kamermans, 2011, Kamermans et al, 2013). These observations suggest that increased SPM loads in the water column may directly (filtration rate) or indirectly (reduced primary production) affect the growth and production of the coastal *Ensis directus* population. Such effects are seen as a negative adverse effects of sand mining and beach nourishment activities which should be evaluated in effect studies.

In order to obtain more insight into determinants of the feeding behavior and growth of *Ensis directus* in natural conditions in the coastal zone, and to validate effects of elevated SPM concentrations, we deployed a measurement platform at 10m water depth off Egmond equipped with a sensor package (turbidity, chlorophyll, T, S, current) and a monitor recording the gape of multiple individuals of (*Ensis directus*). More specifically we asked the following questions:

1. What is the natural variation in silt concentrations close to the seabed

2. what are the forcing factors of this variation
3. is the valve gape of *Ensis directus* related to the SPM concentration.

In 2010 various independent project research groups existed which were all involved in the study of the potential effects of resuspended fine sediments on biota as well as the abiotic environment. One of the initiatives in which NIOZ is involved in is "Building with Nature". For this research program NIOZ did in situ experiments on the potential contribution of *Ensis directus* to the burial of fine sediments in coastal environments. Within this program basic environmental monitoring took place with a limited set of equipment. On request of Rijkswaterstaat and the LaMer foundation the set of instruments for environmental monitoring was significantly increased. Also additional fieldsamples were collected. These sampling locations were the same as those in the MEDUSA project which was supervised by Deltares (Johan de Kok) (de Vries&Koomans, 2010). Additionally, NIOZ also analysed shell- and weight growth of *Ensis directus* which were collected during these MEDUSA cruises between December 2009 and the end of 2010.

To get a better idea of what the signals of the valve gape monitor represent, a deployment of one valve gape monitor with simultaneous growth experiments took place in the NIOZ harbour. The aim was to link valve gape and population averaged growth. The high mortality of *Ensis* in this location however prevented a proper evaluation of the data.

Due to the combination and merging of all the research programs a large and coherent data set could be collected which plays a major role in the section B5 of the evaluation programme of Ellerbroek e.a. 2008.

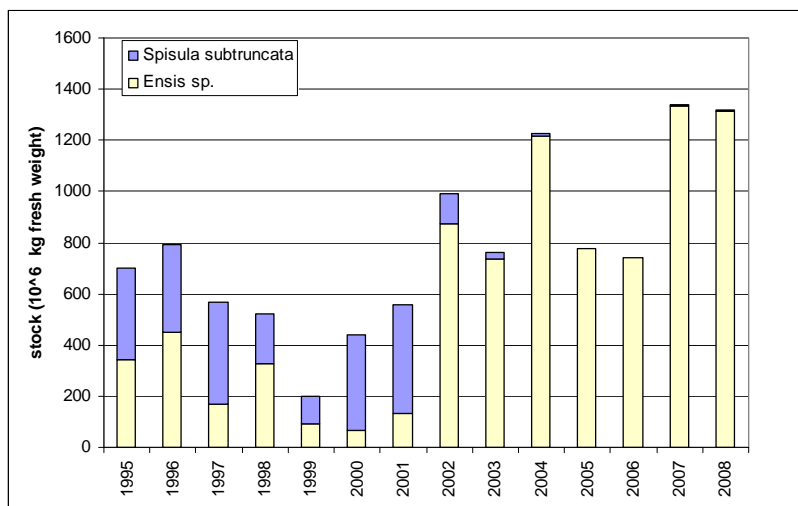


Figure 1. Standing stock of the two most important shellfish species in the Dutch coastal waters in the period 1995-2008 (not published data IMARES; based on yearly stock assessments with modified hydraulic dredge or trawled dredge; sampling efficiency for razor shells estimated at 50%) (Craeymeersch, Perdon, Goudswaard, unpublished).

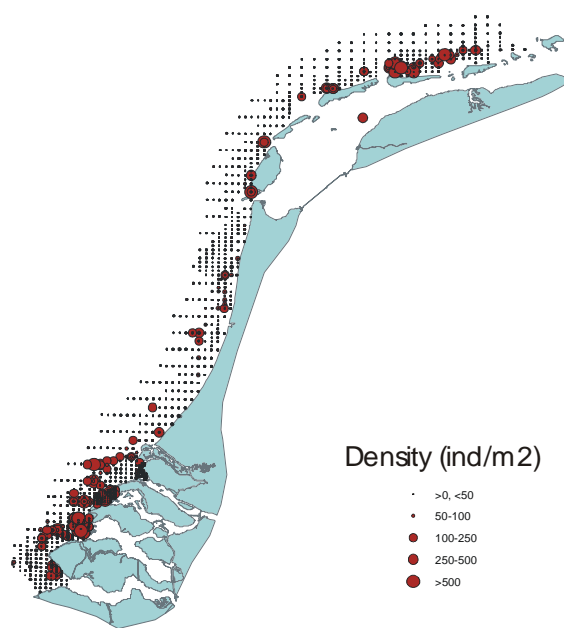


Figure 2. Spatial distribution and density (ind/m²) of *Ensis* sp. in the Dutch coastal waters in the period 1995-2008 (not published data IMARES; based on yearly stock assessments with modified hydraulic dredge or trawled dredge; densities not corrected for 50% sampling efficiency) (Craeymeersch, Perdon, Goudswaard, unpublished)

METHODS

Lander Deployments

The platform which was deployed off Egmond consisted of an triangular aluminium frame (Height Width: 2 x 2 m) with a series ballast weights (total 500 kg) fixed onto the lower support that stands on the seafloor. In this way the center of gravity is lowered as much as possible preventing the platform from falling over during storms. On top of the platform is a pop-up system with a 50-m rope connected to 40 kg floatation. The pop-up is triggered from the surface by 2 acoustic releasers (Benthos). The platform carried 3 closeable mesocosms. These mesocosms are opened (and closed) by means sliding top valves activated with hydraulics. The hydraulics are operated by an ALTRAP pump (Figure 3). Before deployment of the lander, the mesocosms are closed this to prevent sediment to be washed out from the containers carrying live *Ensis*. At preprogrammed time intervals the lids were opened and closed to prevent problems with fouling. The platform carried 1 gape monitor equipped with 8 individuals of *Ensis directus*. (Figure 4).

The platform was further equipped with a series of sensors measuring the following physical parameters: current, temperature, salinity, turbidity and fluorescence. Current speed and direction (3D) were measured every 10 min at 140 cm above the bottom with a NORTEK Aquadopp Doppler current meter. This instrument also yielded a record of the acoustic backscatter. Temperature and Salinity were measured every 10 min with a pumped version of the Seabird SM37 CTD system.

In addition the NORTEK aquadopp current meter a NORTEK Vektor current meter was mounted at the lander at a height of 30 cm above the bottom. Every 10 minutes this instruments made high frequency burst measurements during 2 minutes with a frequency of 1/second. Turbidity and fluorescence were measured optically at four heights above the bottom, i.e. 30, 120, 150 and 200 cm, using ALEC Compact-CLW's

with wipers. The measurement at the lowest height (30cm) was done with the infinity version of the instrument as it can deal with higher turbidity. The wiped versions appeared all to be crucial for obtaining optic records in coastal environments with heavy fouling. An overview of the instruments and the mounting heights on the lander above the bottom is given in Table 1. Overview of the instruments mounted on the lander, position and the variables measured.

Table 1. Overview of the instruments mounted on the lander, position and the variables measured.

Height	Measured variable	Height above seafloor
Vektor current meter	Current speed, Direction and pressure	30 cm
Aquadop current meter	Current speed & Direction	140 cm
CTD	Salinity and Temperature	140cm
Alec	Fluorescence and Turbidity	30,120,150,200cm
Valve gape monitor	Valve gape (percentage)	30-45 cm

After retrieval of the lander the measurement platform was serviced, the data downloaded and the instruments subsequently reprogrammed. This normally took 1 full day of work while the ship was moored in the harbour of IJmuiden. Main reason was that there was only 1 set of instruments available. The position of the platform (Figure 5, Figure 6) was marked by two buoys protecting it from trawling activity. In 2010 the lander was deployed during two three week periods in spring as well as in autumn. In Table 2 an overview of the deployment and retrieval dates is given.

Table 2. Overview of deployment dates and ships used in the project in combination with BWN

Deployment nr.	Start Date	End Date	Ship
1. Week 10_14	12/03/2010 18:00	06/04/2010 16:00	Navicula
2. Week 14_17	09/04/2010 18:00	26/04/2010 16:00	Navicula
3. Week 37_41	16/09/2010 18:00	12/10/2010 12:30	Navicula
4. Week 41_44	13/10/2010 20:00	01/11/2010 15:40	Navicula

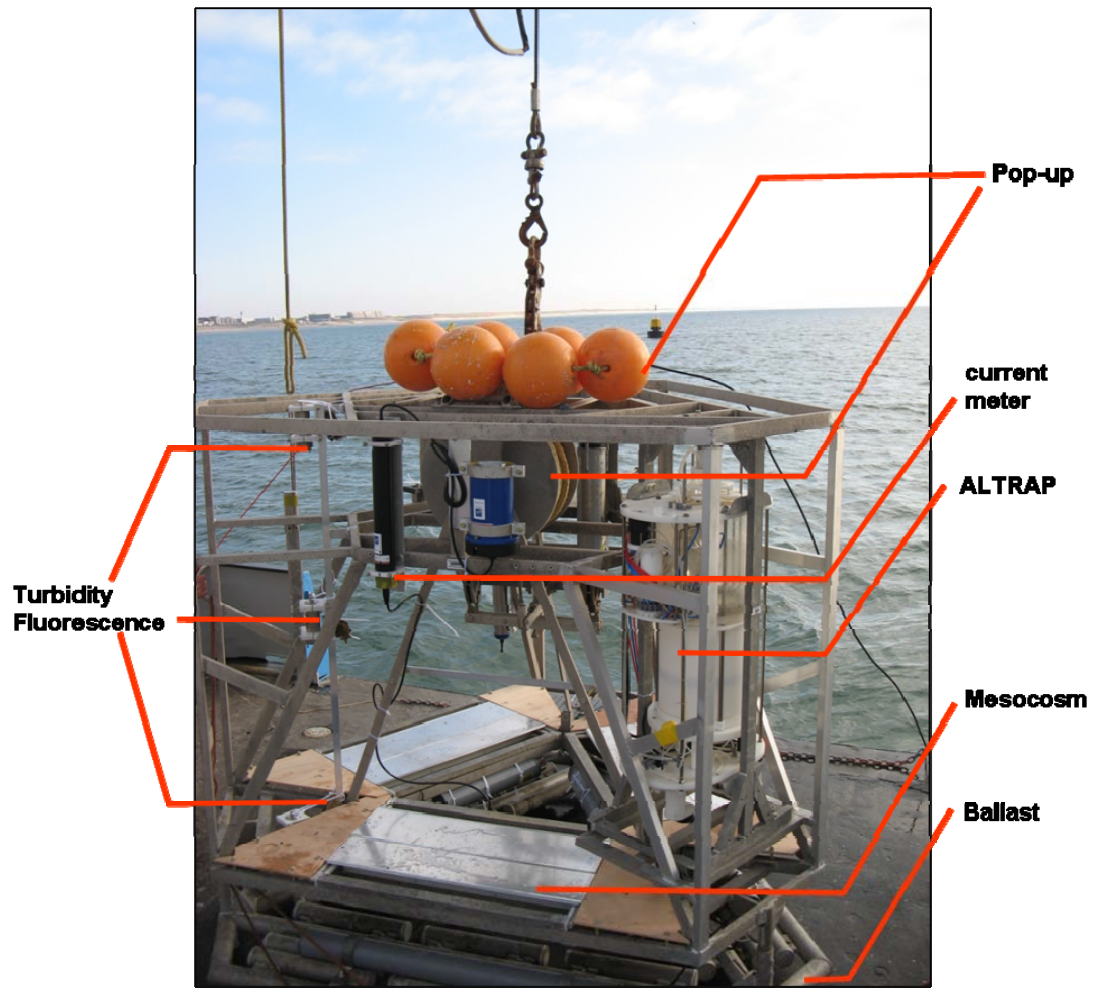


Figure 3. Overview of one the lander frames used in the environmental monitoring off the coast of Egmond in 2011.



Figure 4. Placement of sediment cores with live *Ensis* connected to a valve monitor in one of the trays which are mounted on the lander.

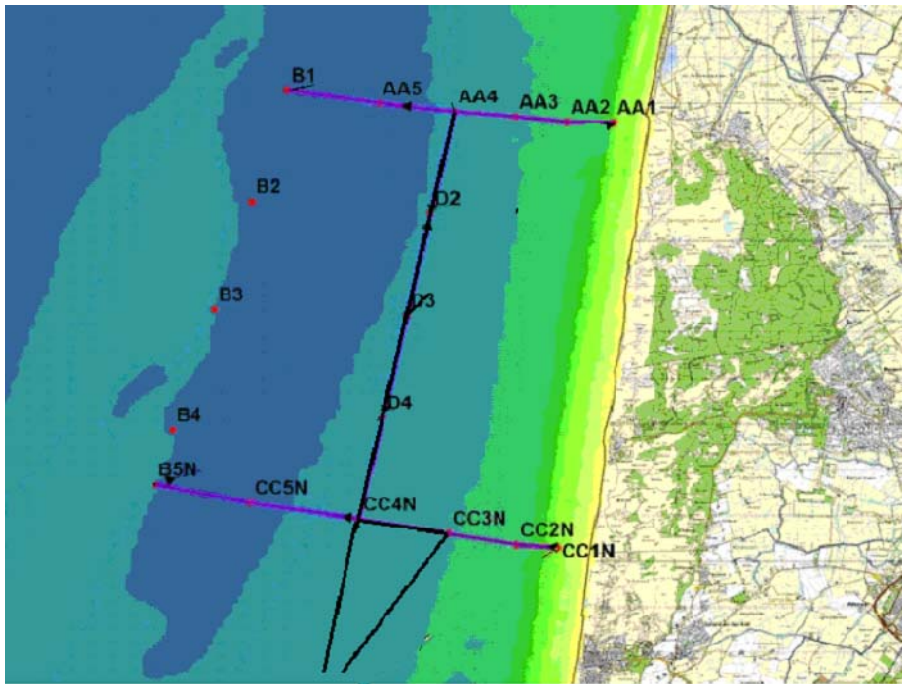


Figure 5. Map with stations as being sampled by Medusa (Johan de Kok). The lander position is just south east of station cc2N.

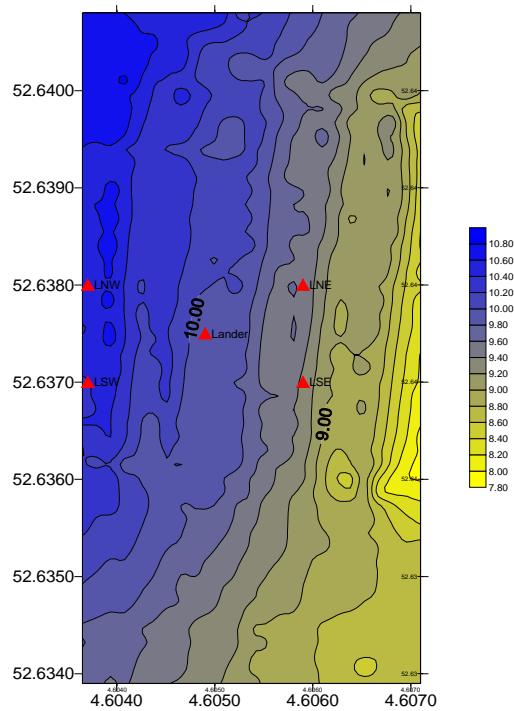


Figure 6. Lander and boxcore stations overlaid on a depth contour map made of the area in June 2013 on basis of ADCP depth profiling of the area.

Valvometry

The deployed lander platform carried 1 gape monitor equipped with *Ensis directus*. This instrument simultaneously measured the gape of 8 of these bivalves at frequency of 1 measurement in three minutes. The gape distance is measured by means of the inductive current generated through a pair of micro-coils which are glued to the valves.

The *Ensis* were placed in pvc tubes which were hosted in a tray like construction. During the actual deployment operation of the lander this tray was closed with a lid to protect the sediments in the experimental set up of being washed away. Furthermore were the lids on the "trays" programmed to open and close once a day to prevent that fouling inhibits the closure of the trays at the end of the deployment when the lander had to be retrieved. The height at which the gape monitor was placed on to the lander was within the measuring range of the lowest placed turbidity sensor, i.e. 30-45 cm above the bottom. As far as possible, the same animals were used again in following deployment period. This was attempted in both the spring as well as the autumn sampling. In practice the high mortality of *ensis* limited this to a large extent.

Additional sampling

During each service operation two additional boxcore samples at four corner locations around the central lander position were taken (see Table 3). From each of these boxcores a subcore for sediment grainsize analyses was preserved. The remainder of the boxcore was sieved over a 1 mm screen and the live *Ensis* were collected and stored for size measurements and ash free dry weight determination. In this way a time series of the growth and population development of the local *Ensis* stock is obtained. In addition to these box core samples additional boxcore samples were taken along a transect perpendicular to the coast and similar to the locations as being sampled in the Medusa project by de Kok. *Ensis* samples collected by Medusa explorations were brought to NIOZ for measurement and Ash free dry weight analyses. For an overview of approximate locations see (Figure 5, Figure 6) and Table 3 and Table 4.

Table 3. Positions around the central position at where boxcore samples are taken to follow the seasonal development of sediment grainsize and to follow the wax and wane of the local Ensis population.

station	gr min decmin N	gr min decmin E
LSE	52 38 28	4 36 356
LZO	52 38 216	4 36 380
LZW	52 38 22	4 36 22
LNW	52 38 281	4 36 22

Table 4. Positions along the "MEDUSA" transects perpendicular to the coast. At each location two boxcore samples were taken. From each boxcore one sub core for sediment grain size was collected. Living Ensis were kept for analyses in the lab.

Station	Latitude gr min decmin	Longitude gr min decmin
AA1	52°43.4590'N	04°37.7380'E
AA2	52°43.4600'N	04°36.8680'E
AA3	52°43.5170'N	04°35.9080'E
AA4	52°43.5730'N	04°34.7640'E
AA5	52°43.6570'N	04°33.3440'E
B1	52°43.8010'N	04°31.6270'E
B2	52°42.4850'N	04°30.9870'E
B3	52°41.2090'N	04°30.3130'E
B4	52°39.7870'N	04°29.5600'E
B5	52°39.1426'N	04°29.2349'E
D2	52°42.36987'N	04° 33.48963'E
D3	52°41.16676'N	04° 33.91406'E
D4	52°39.96362'N	04° 34.33888'E
C1	52°38.4513'N	04°36.7757'E
C2	52°38.4811'N	04°36.0116'E
C3	52°38.6029'N	04°34.7456'E
C4	52°38.7605'N	04°33.0655'E
C5	52°38.9378'N	04°31.0345'E

Lab procedures

Ash Free dry weights.

During transport to the lab all collected animals were kept under refrigeration. The *Ensis* collected by Medusa explorations were supplied to NIOZ in frozen condition although a note has been made by the project leader of Medusa that one sample set got defrosted and was successively frozen again. From each individual shell, total length, width and thickness were measured. In case shell length was not complete, shell length was reconstructed on basis of the regression relationship between shell width and length.

From all complete individuals the soft tissue was separated from the shell. Soft tissue was dried at 60°C until constant and from the difference from this dry weight and the remaining ash after incineration at 540°C, the ash free dry weight was calculated. Compared to using dry weights the ash free dry weights have a smaller error as it corrects for inorganic sediments enclosed within the soft tissues.

The data from the quantitative boxcores samples together with the size and weight measurements gives insight in population changes over time as well as average growth. Almost 2800 *Ensis* were treated in this way.

RESULTS.

Ensis directus

For 15 dates between September 15th 2009 and December 23rd 2010, about 2791 *Ensis* were collected from the Medusa transects and from the locations around the lander. The length frequency data suggest that over this period of sampling three *Ensis* size cohorts (Figure 7; Figure 8) are present in the area. Data on average density, biomass and size are given in Table 5.

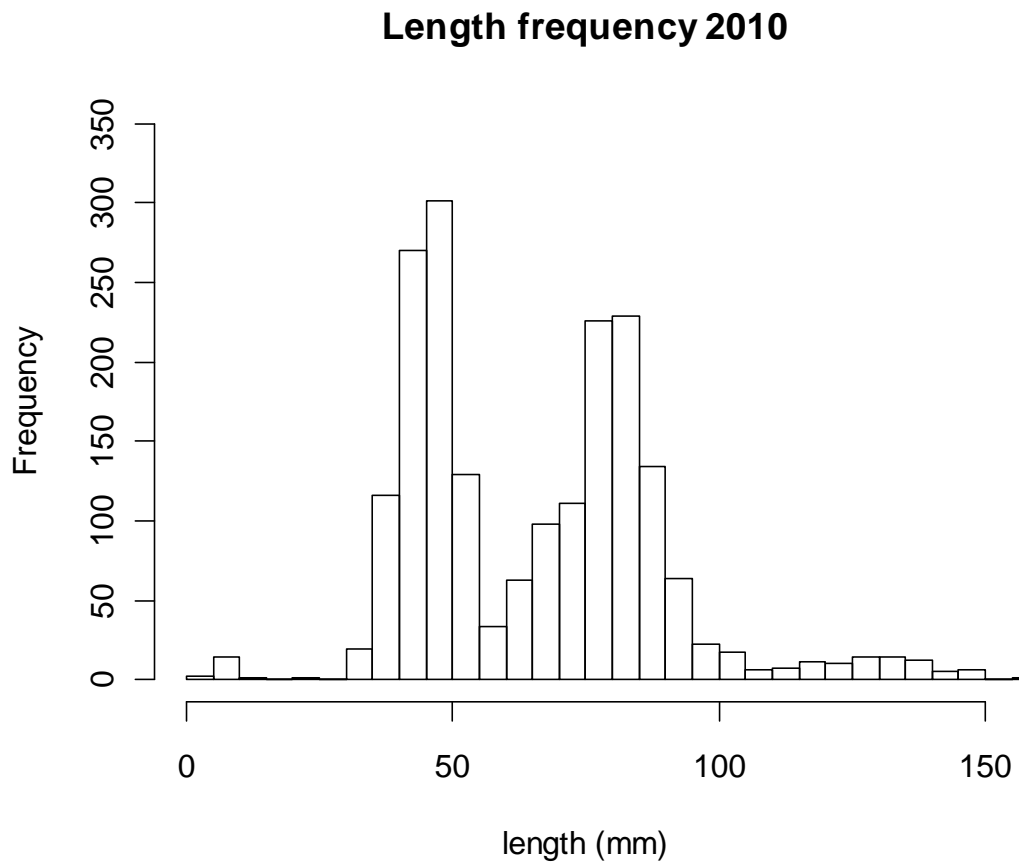


Figure 7. Length frequency distribution of pooled samples collected from different locations and sampling dates.

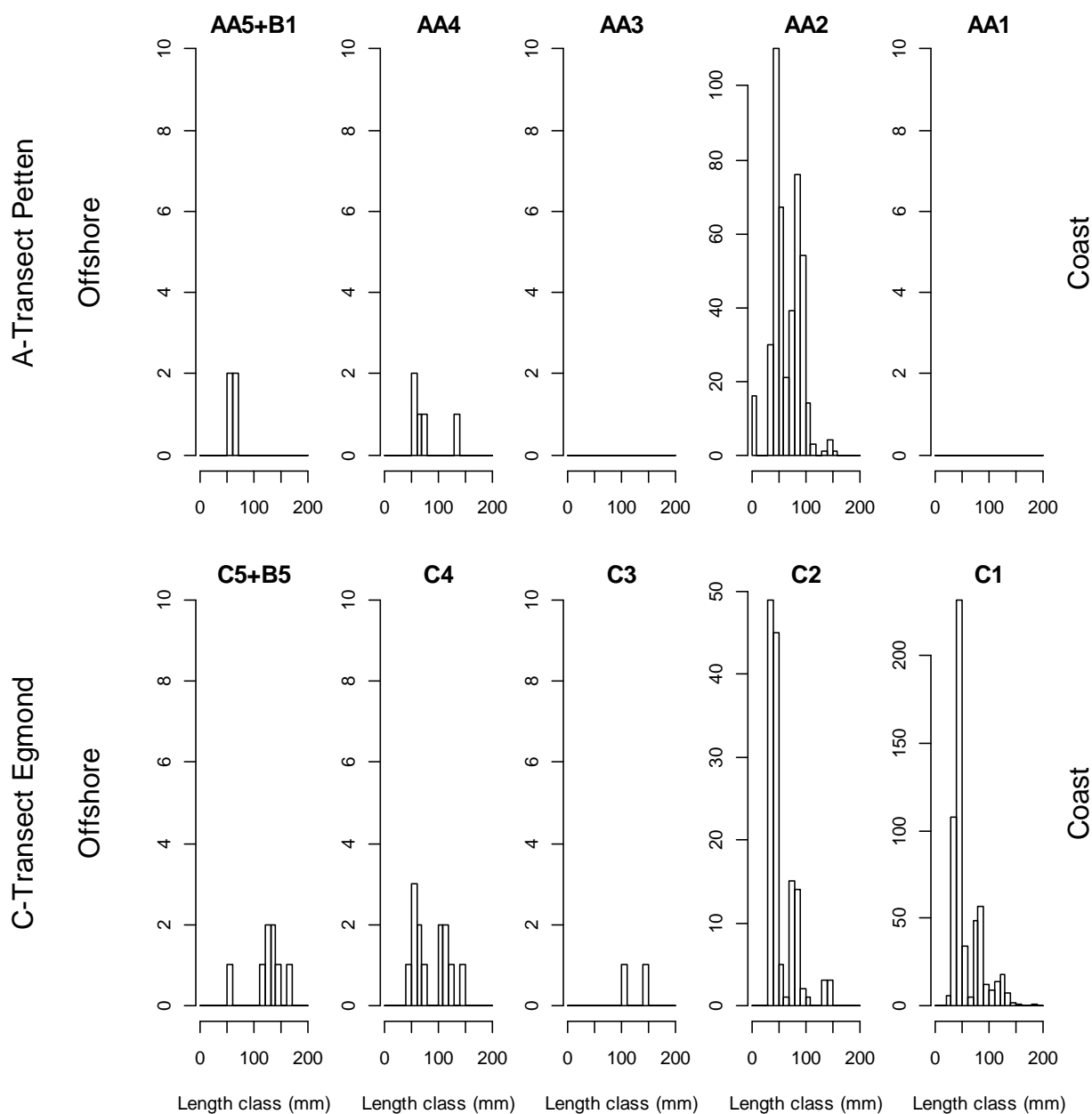


Figure 8. Length frequency distributions of *Ensis directus* lengths in 2010 at different locations at the southern and northern transect (Fig 5). The coastal stations lie about 1 km from the beach and have a water depth of approximately 10 meter. Because densities at the most offshore locations (AA5+B1, C5+B5) were too low, the data collected at the outermost stations were pooled to generate a length frequency distribution.

Table 5. Key features of the *Ensis directus* population as sampled in 2010 across the coast.

Station	mean Length (mm)	mean AFDW / animal	Dens N/m ²	AFDW gr/m ²
AA1	0.00	0.00	0.00	0.00
AA2	57.13	0.24	335.81	80.59
AA3	39.50	0.00	243.20	0.00
AA4	75.83	0.43	23.04	9.98
AA5	0.00	0.00	0.00	0.00
B1	59.40	0.20	17.07	3.41
B2	0.00	0.00	0.00	0.00
B3	0.00	0.00	0.00	0.00
B4	0.00	0.00	0.00	0.00
B5N	0.00	0.00	0.00	0.00
CC1	0.00	0.00	0.00	0.00
CC2	58.55	0.25	371.20	92.80
CC2N	58.79	0.19	708.80	137.03
CC3	134.00	1.60	34.13	54.61
CC4	47.07	0.07	6.40	0.43
CC4N	75.20	0.45	1241.60	558.72
CC5	0.00	0.00	0.00	0.00
D2	136.00	0.00	8.53	0.00
D3	0.00	0.00	0.00	0.00
D4	135.00	2.80	19.20	53.76
LNO	86.18	0.62	104.96	65.08
LNW	77.32	0.46	330.24	151.91
LZO	81.46	0.56	245.76	137.63
LZW	77.47	0.55	292.27	160.75

In 2010 the size of the sampled animals ranged between 5 and 182 mm. Maximum density was found at station CC4 during a "Medusa" sampling campaign and was as high as 1240 individuals/m². These high densities were never encountered during NIOZ (BWN) sampling campaign in the same year.

With 103 individuals/m² the *Ensis directus* densities at the northern transect "A" are significantly lower when compared to the southern "C" transect where the densities (including the lander stations) was 303 individuals/m². Average density measured over all stations, i.e. also the stations where no *Ensis* were found is 265 individuals/m². Going from inshore to more off shore locations the densities decrease. Peak densities

along both transects are found around the 10 meter depth contour (AA2 & CC2-Lander) (Figure 9). Along these transects the average size of the animals is bigger at the stations further away from the coast, which is related to the presence of older cohorts further away from the coast.

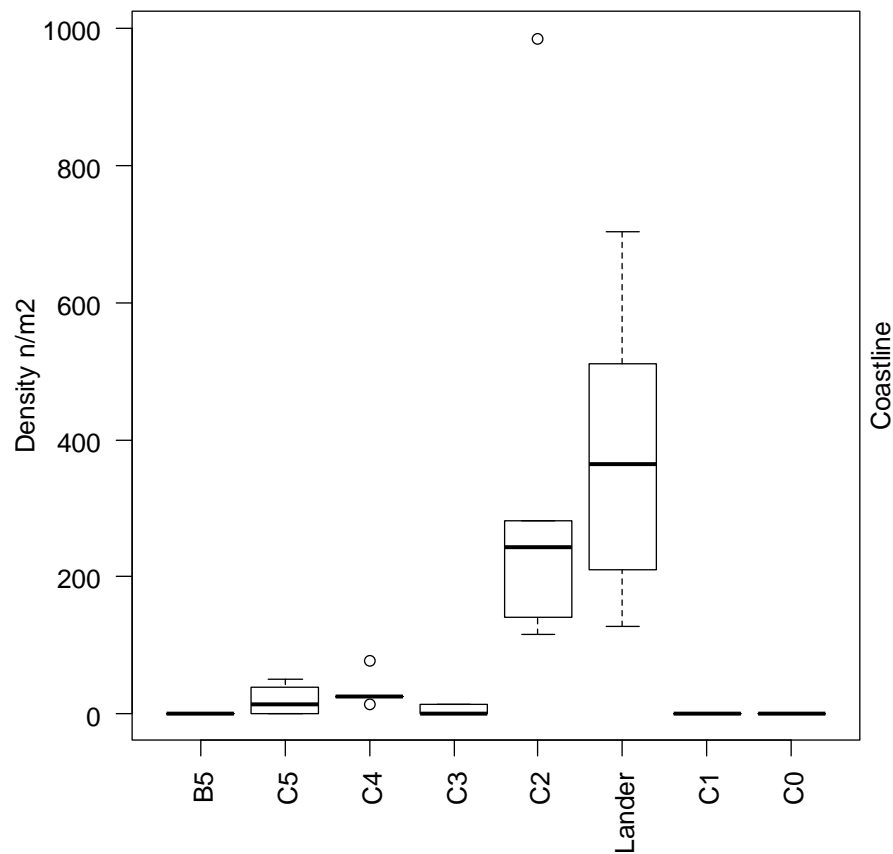


Figure 9. Box of the Ensis densities across the southern (C) transect.

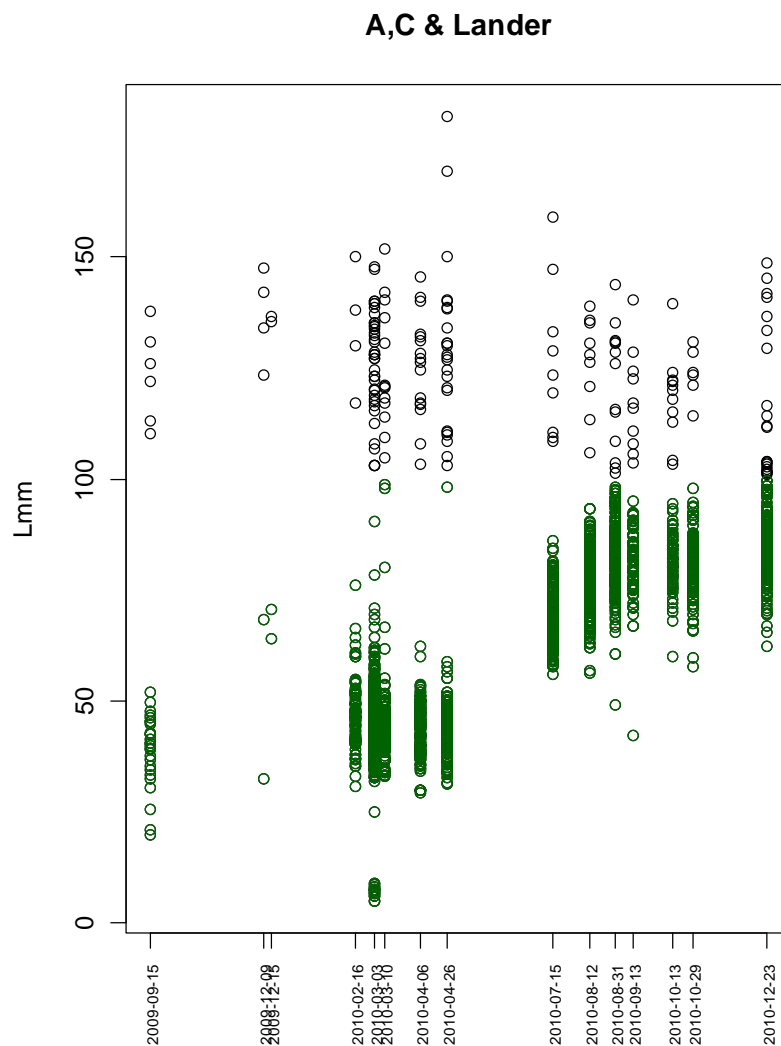


Figure 10. Dotplot of the *Ensis* shell lengths over time. The cohort which settled in 2009 is marked with green symbols.

In Figure 10 the lengths of all *Ensis* caught over all stations is depicted as dotplot. The cohort which settled in 2009 and which had an average length of ~40mm in September 2009 is marked green and can be followed over time. The graph suggests that main shell growth took place between the end of April and mid July. Unfortunately no sampling took place in that period. In Figure 11 size frequency histograms by collection date are given together with a summarizing boxplot (Figure 12).

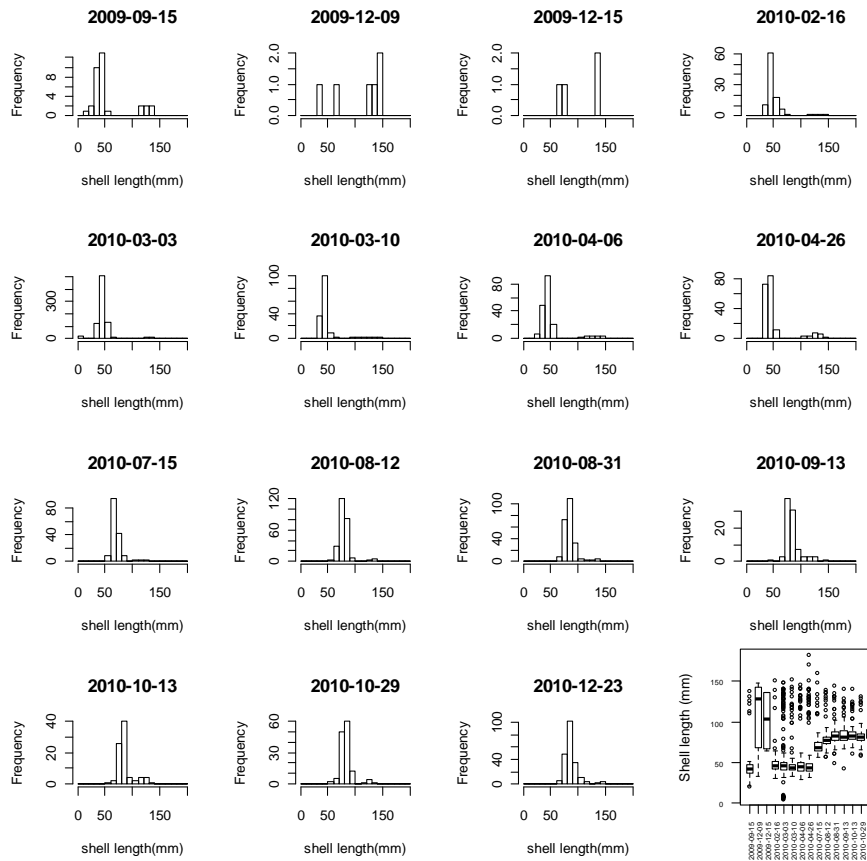


Figure 11. Size distribution of all the collected *Ensis* of all samples pooled by collection date.

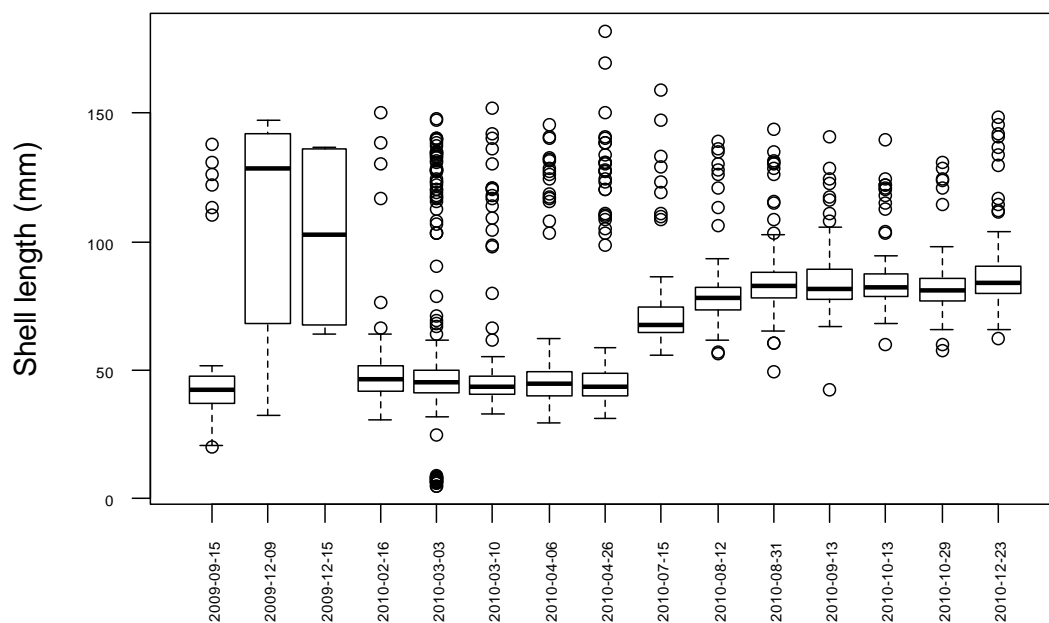


Figure 12. Enlargement of the boxplot (Shell length X Collection date) as given in figure 11.

Weight and condition

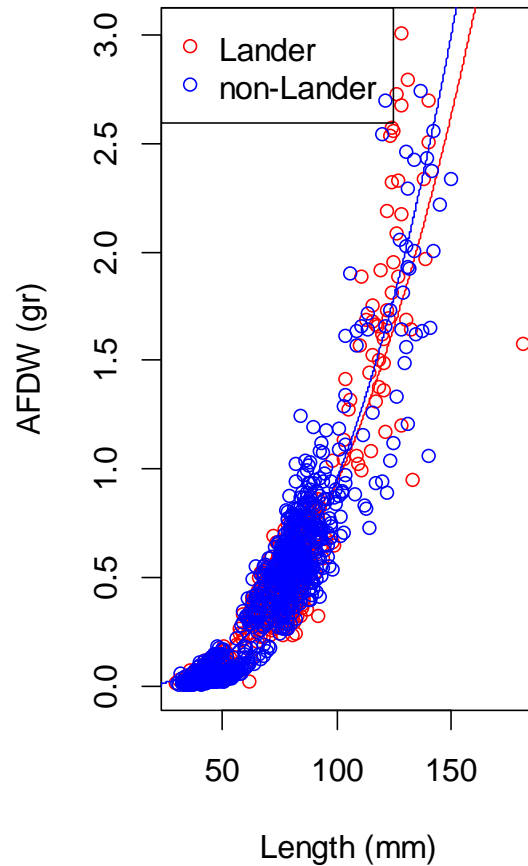


Figure 13. Length - Weight relationship of all *Ensis* which were collected along the transects (blue dots) and around the lander (red dots). No difference existed in the length weight relationship of the two "sample populations" ($P > 0.47$)

The relationship between Shell length (mm) and Ash Free Dry Weight (gr) for *Ensis* irrespective of collection station is highly significant ($P < 0.001$).

$$\text{AFDW} = 4.074 \times 10^{-6} \times \text{Length}^{2.684}$$

Comparison of the regressions between weight and Length for each of the sampled groups (Lander - non Lander, Figure 13) did not differ from each other. This suggests that the weights at the locations around the lander are similar to those collected over the wider area, i.e. the transects.

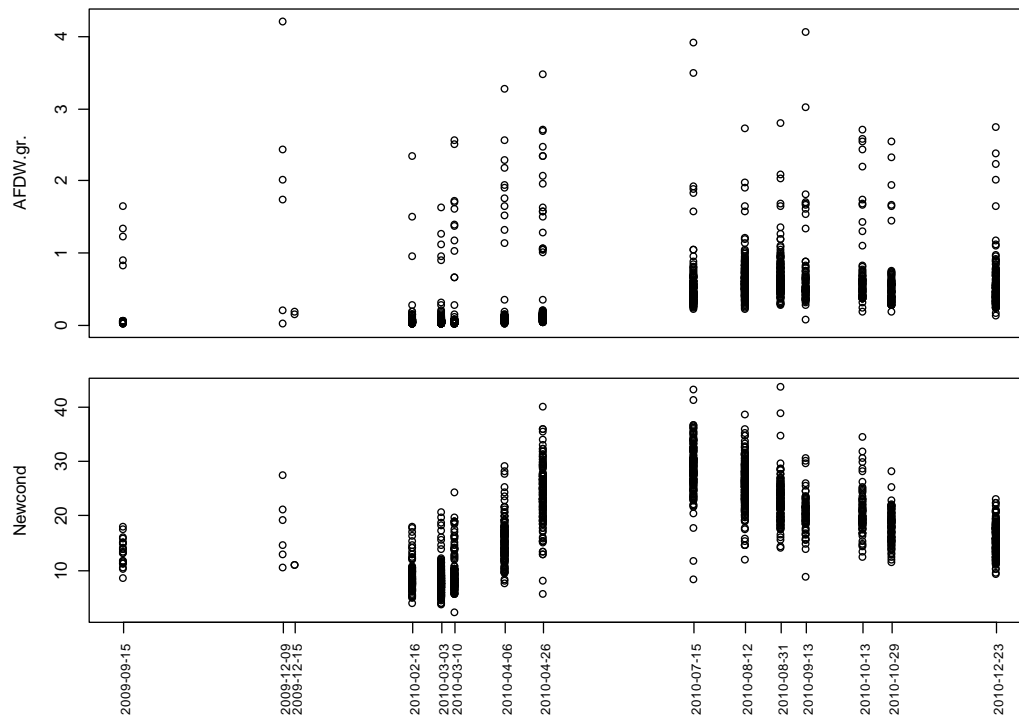


Figure 14. Seasonal development of Ash Free dry Weight and condition index..

In Figure 14 the seasonal development of the ash free dry weights and condition index of all animals shows that maximum condition of the animals in 2010 was found between the end of April and mid July. After mid July condition indices tend to decrease.

Environmental Data.

Temperature and Salinity

Figure 15 gives the temperature and salinity measured at 5 to 10 minute intervals over the two experimental periods (spring & autumn).

Temperature ranged between ~ 4.0 and $17 \sim \text{deg } ^\circ\text{C}$. Salinity ranged between 26 and 32.4 per mil. Both parameters show a well defined tidal cycle which is present all over both measurement periods.

The average daily variation in temperature amounts $1.2 \text{ } ^\circ\text{C}$. In salinity the average daily variation is about 1 %.

Table 6

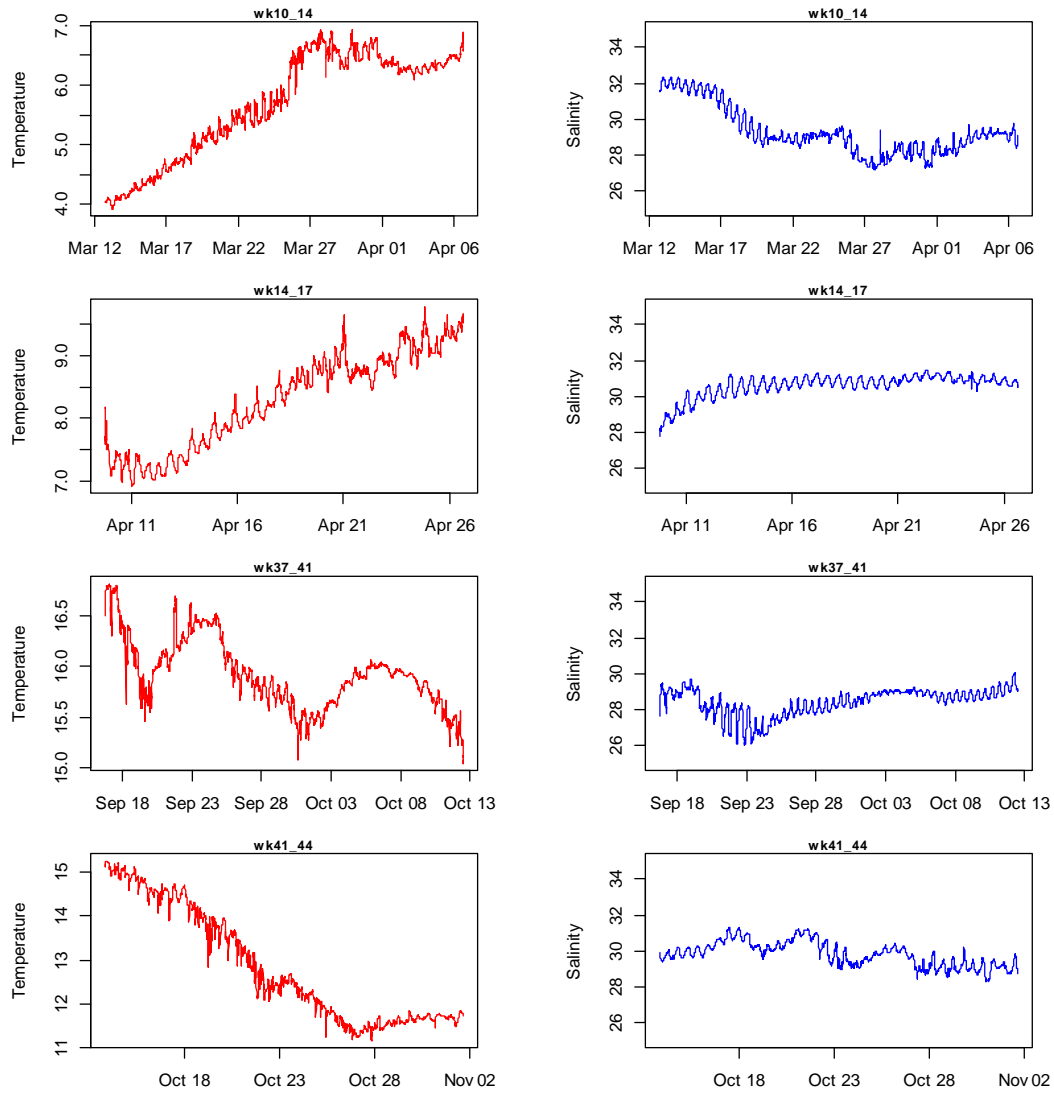


Figure 15. Salinity and temperature development up to 27 September 2011.

Table 6. Key values for Salinity and Temperature extracted for the spring and autumn lander deployment period.

	max. temp	mi n. temp	max. sal	mi n. sal
wk10_14	11.84	9.16	32.36	27.18
wk14_17	12.53	9.02	31.46	27.77
wk37_41	11.95	9.20	30.06	26.01
wk41_44	12.06	9.15	31.31	28.31

Currents.

Figure 16 summarizes the measured current data by measurement period as a series of vektor plots. In spring 2010 the residual current had a southerly direction. In autumn the residual current has a northward direction. Maximum current speeds of slightly over 1 m/s were measured in autumn. The figure also illustrates that the current speeds in autumn 2010 are slightly higher when compared to those measured in spring 2010. This apart from the directional change. Key values for the current velocities and directions are given in Table 7.

Table 7. Key values (velocity in m/s) of two current vectors (North & East) measured at 140 cm above the seafloor. Given are minimum and maximum currents measured in each of the measurement periods.

Period	max.North	min.North	max.East	min.East	avg.speed	max.speed
wk10_14	0.62	-0.51	0.15	-0.29	0.19	0.62
wk14_17	0.53	-0.54	0.35	-0.44	0.24	0.54
wk37_41	0.8	-0.63	0.32	-0.24	0.27	0.8
wk41_44	1.01	-0.76	0.41	-0.41	0.25	1.03

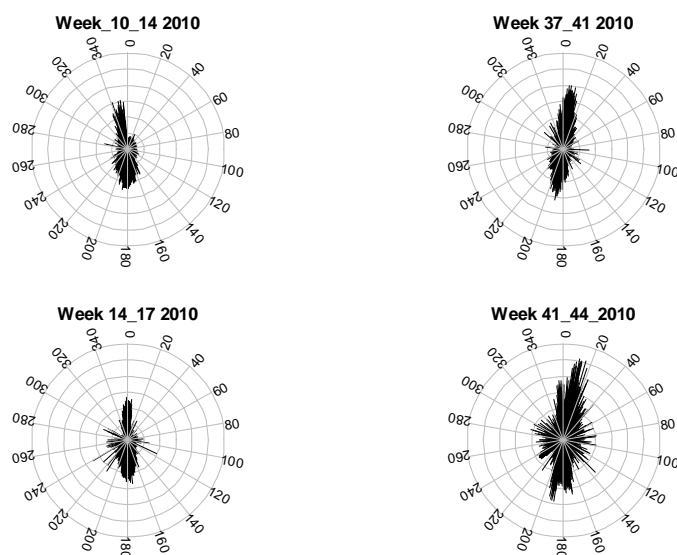
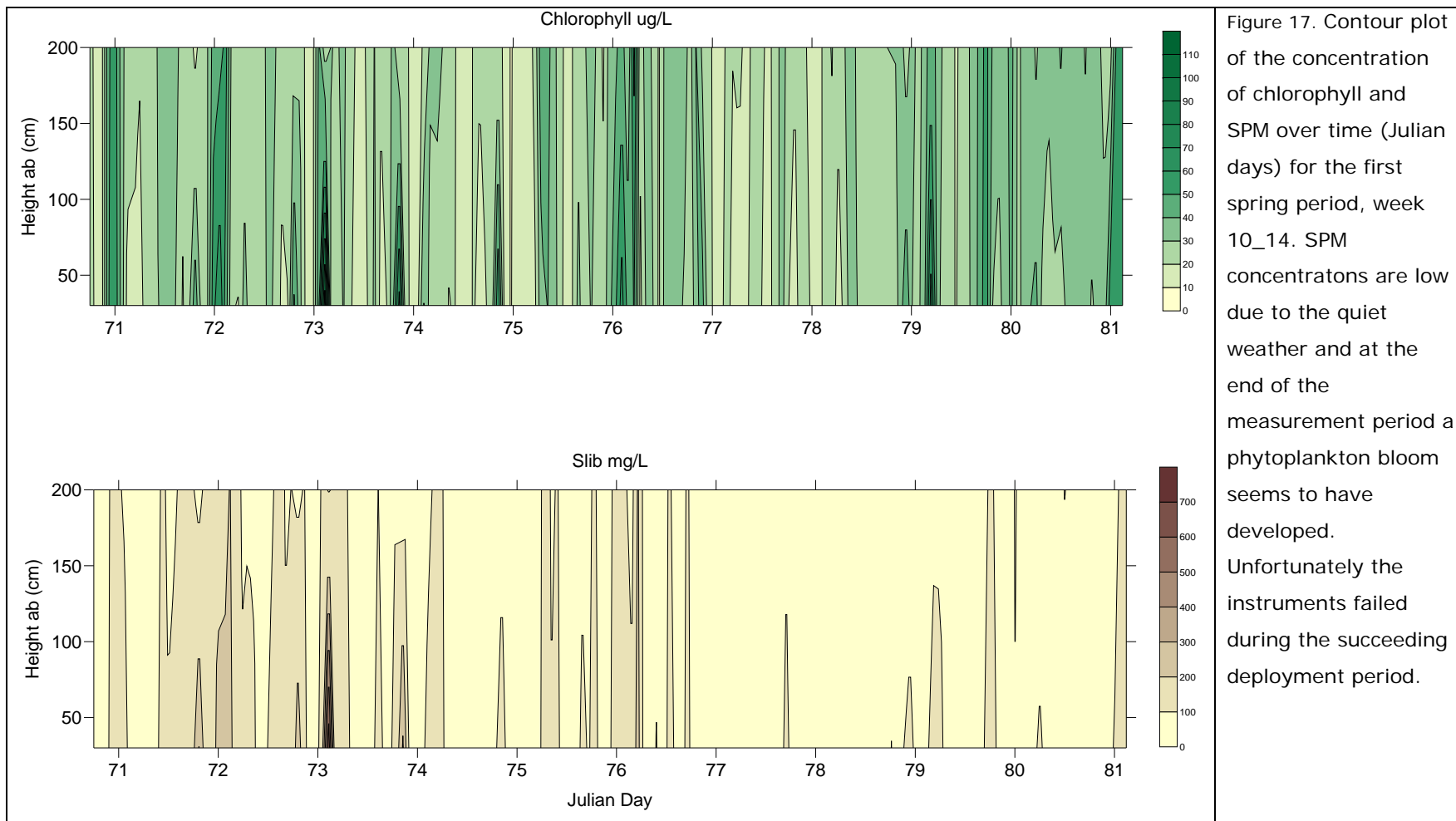


Figure 16. Vector plots of current direction and strength by measurement period. Radial grid steps is current speed in steps of 0.2 m/s. Outer circle is maximum speed of 1.2 m/s. Labels around outer circle is current direction in degrees. All 10 minute measurements taken in a period are given in the vector plot.

Suspended matter.

Optical backscatter and fluorescence was measured at four heights above the bottom. The day to day variation as well as differences between the four measurement heights have been visualized as contour plots in Figure 17 (Spring period) and ~~Figure 18~~ (autumn period). Key values such as daily mean concentrations are given in Table 8. In the spring period an average of about 100mg/L is found. In the autumn the average concentrations range between 250 and 300 mg/L. But much higher maximum SPM peak concentrations of almost 4000 mg/l and 2925 mg/l were measured in the autumn periods at 30 cm above the seafloor. The huge within day variation as well as day to day variation is illustrated by the high standard deviations around the daily averages (Table 8). A maximum Chl-a concentration of 108 ug/l was measured in the March period probably associated with the start of the spring bloom. In this period the average chlorophyll concentrations are 4 to 5 times higher when compared to those measured in autumn. In autumn the high chlorophyll concentrations are most likely associated with the inorganic fine sediment fraction.

For all measurement periods, especially the vertical distribution SPM is distinct. The ratio between the SPM measured at a height of 30 cm and at 200 cm above the seafloor shows that close to the seafloor the concentration can be 85 times higher when compared to the concentrations at 200 cm above the bottom. This height difference is less pronounced for ratio Chlorophyll measured at 30 and 200cm above the seafloor (Table 9). The time evolution of the chlorophyll and SPM concentrations (~~Figure 18~~) suggest that at least for autumn high chlorophyll concentrations are linked to resuspended sediments.



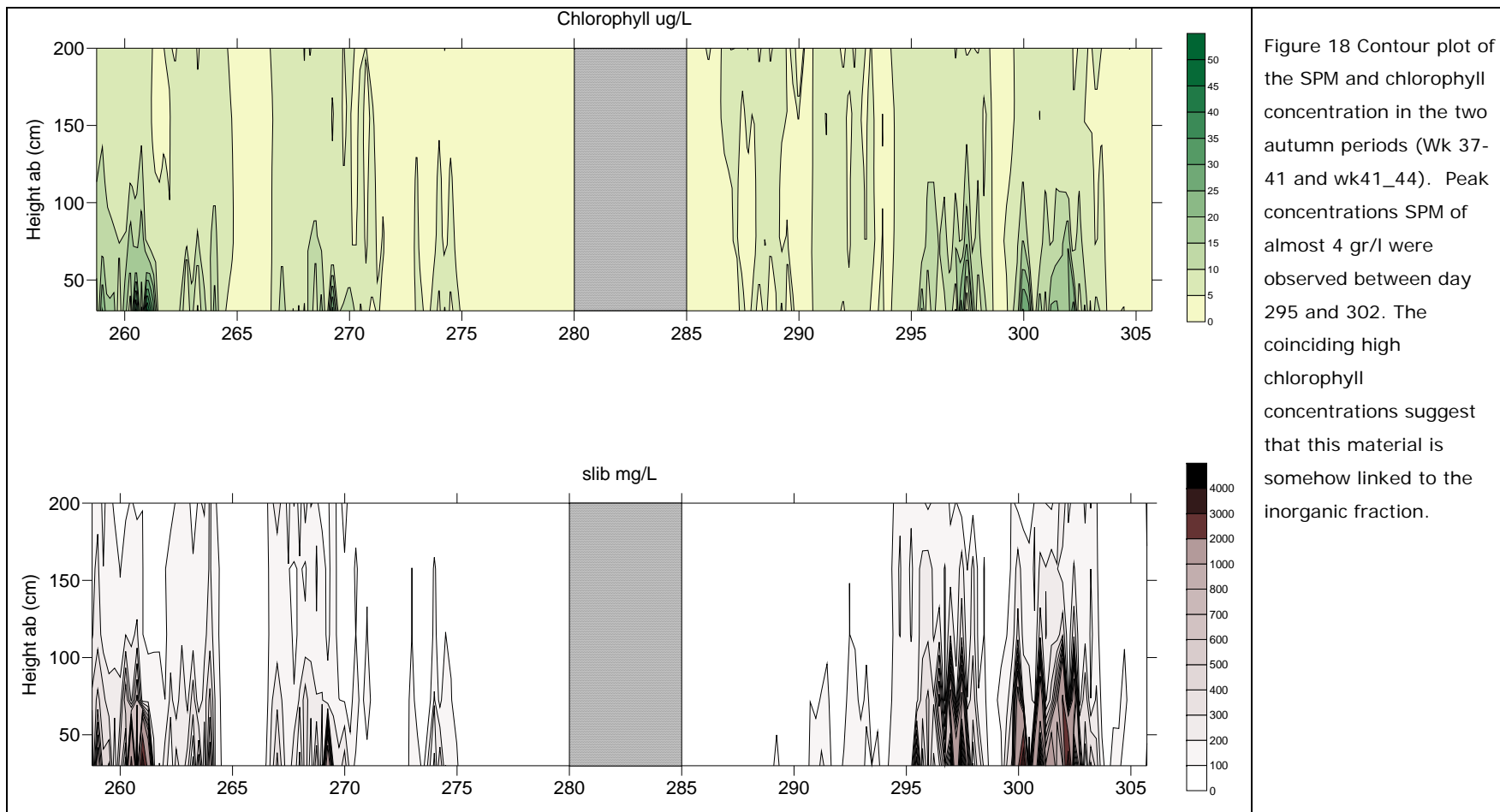


Figure 18 Contour plot of the SPM and chlorophyll concentration in the two autumn periods (Wk 37-41 and wk41_44). Peak concentrations SPM of almost 4 gr/l were observed between day 295 and 302. The coinciding high chlorophyll concentrations suggest that this material is somehow linked to the inorganic fraction.

Table 8. Key values (concentrations) of chlorophyll and SPM (mud) measured at four heights above the bottom in the three measurement periods.

	Height cm.	wk10_14		wk37_41		wk41_44	
		daily		daily		daily	
		mean	sd	mean	sd	mean	sd
SPM mg/L	200	76.8	29.8	66.4	38.2	69.3	35.9
SPM mg/L	150	-	-	87.5	52.0	94.4	49.8
SPM mg/L	120	-	-	83.3	50.3	88.4	49.9
SPM mg/L	30	99.1	47.3	246.7	273.2	307.3	337.7
Chl-a ug/L	200	29.2	9.0	5.1	1.1	5.3	1.1
Chl-a ug/L	150	-	-	5.0	1.2	5.6	1.2
Chl-a ug/L	120	-	-	5.5	1.6	5.7	1.5
Chl-a ug/L	30	30.6	11.9	8.1	4.3	8.1	4.3

Table 9. Ratio of chlorophyll and SPM (mud) measured at 30cm above the bottom and 200 cm above the bottom.

Type	Period	Min	Mean	Max.
Ratio chl/SPM 30cm	wk 10-14	0.135	0.330	0.732
Ratio chl/SPM 30cm	wk 37_41	0.009	0.077	0.690
Ratio chl/SPM 30cm	wk 41_44	0.005	0.117	1.975
Ratio chl/SPM 200cm	wk 10-14	0.194	0.405	0.890
Ratio chl/SPM 200cm	wk 37_41	0.022	0.131	0.960
Ratio chl/SPM 200cm	wk 41_44	0.029	0.195	2.560

The ratio of chlorophyll to total suspended matter (mud) can be regarded as a measure for the quality (as food source) of the suspended matter. The data show that there is a marked seasonal difference between these ratio's as is shown in Figure 19

and shows that in early spring the slope between both parameters is very steep when compared to those measured in autumn.

The gradual increase of the chlorophyll/SPM ratio with time, indeed suggest that during the first measurement period a gradual built up of phytoplankton biomass takes place (Figure 20). On a shorter time scale the ratio close to the bottom is closely coupled to the variations in tidal currents, i.e. increasing ratios with decreasing current speeds (Figure 21; Figure 22).

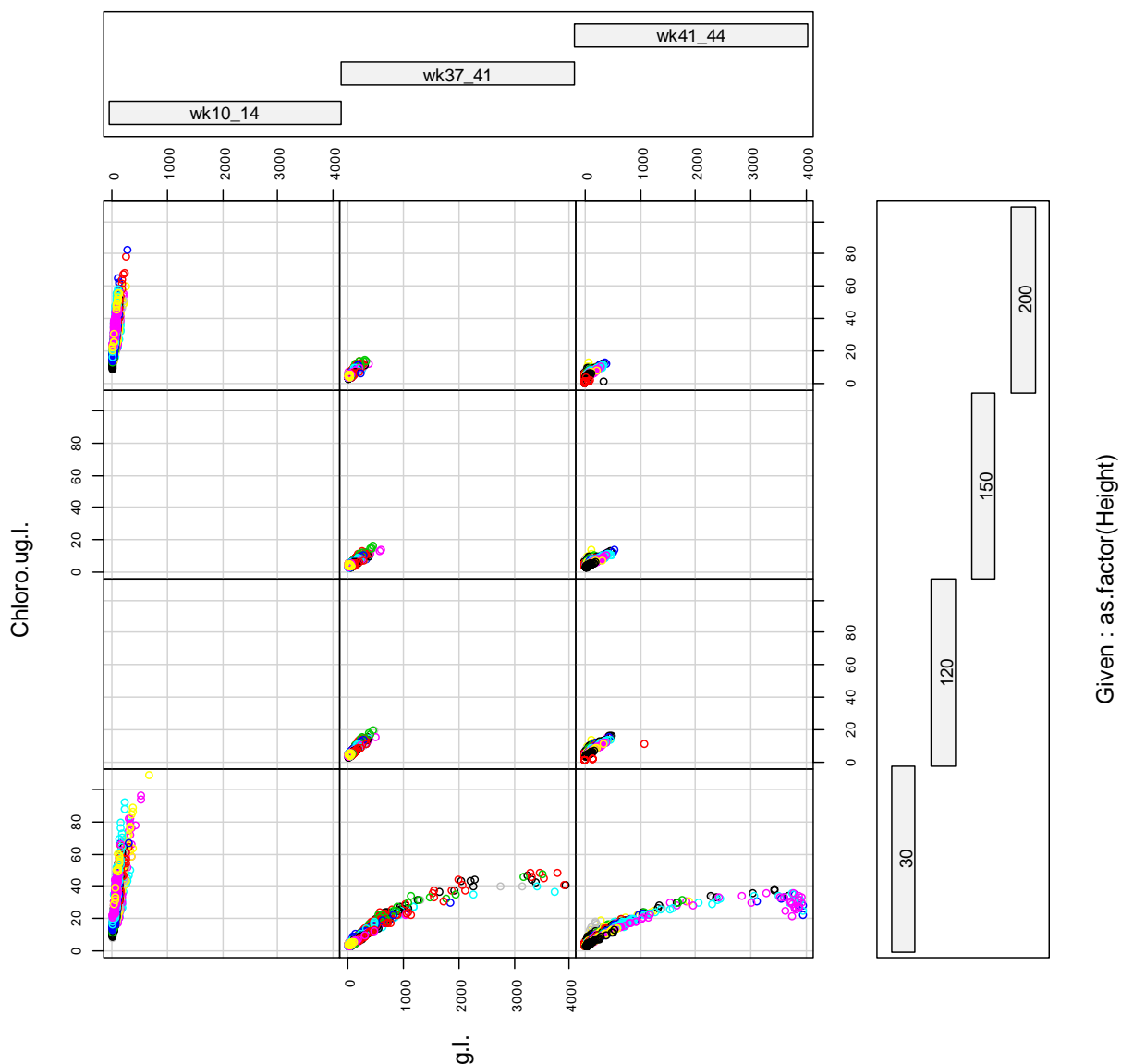


Figure 19. Plots of chlorophyll concentration (Y-axis) being dependent on the SPM concentration. Panel column from left to right represent the three measurement periods. Panel rows represent the height above the seafloor. Colors represent measurements taken at the same day. All collected data have been used to generate the plot.

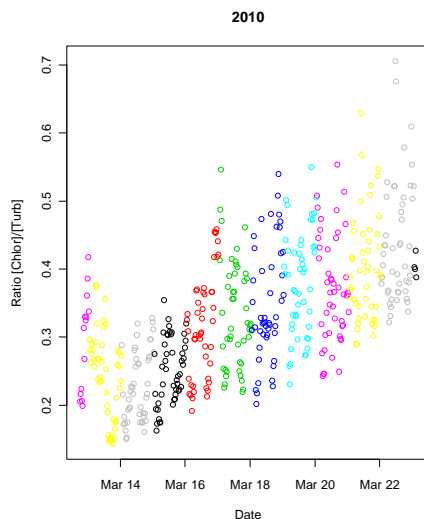


Figure 20. The gradual increase of the ratio of chlorophyll to SPM (mud) over time.

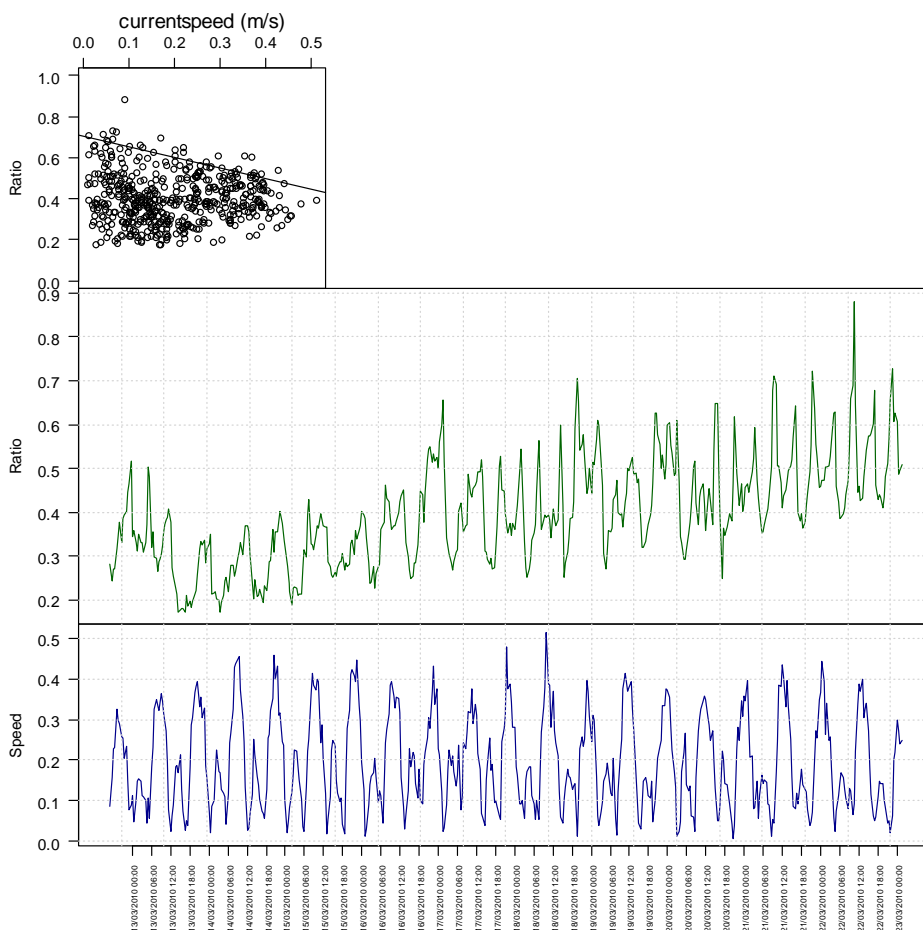


Figure 21. The top panel gives the ratio chlorophyll to SPM (mud) in relation to current speed in spring. The regression line is the .95 quantile regression. The lower panels give Ratio of Chl-a to SPM in green and the current speed (blue). The highest ratios are found at slack tide when current speed is minimal. This demonstrates that the food availability and food quality for the local *Ensis* population varies strongly over the tidal cycle. With the progress of the season (spring bloom) the quality increases as can be derived from the trend in the Ratio (Figure 19)..

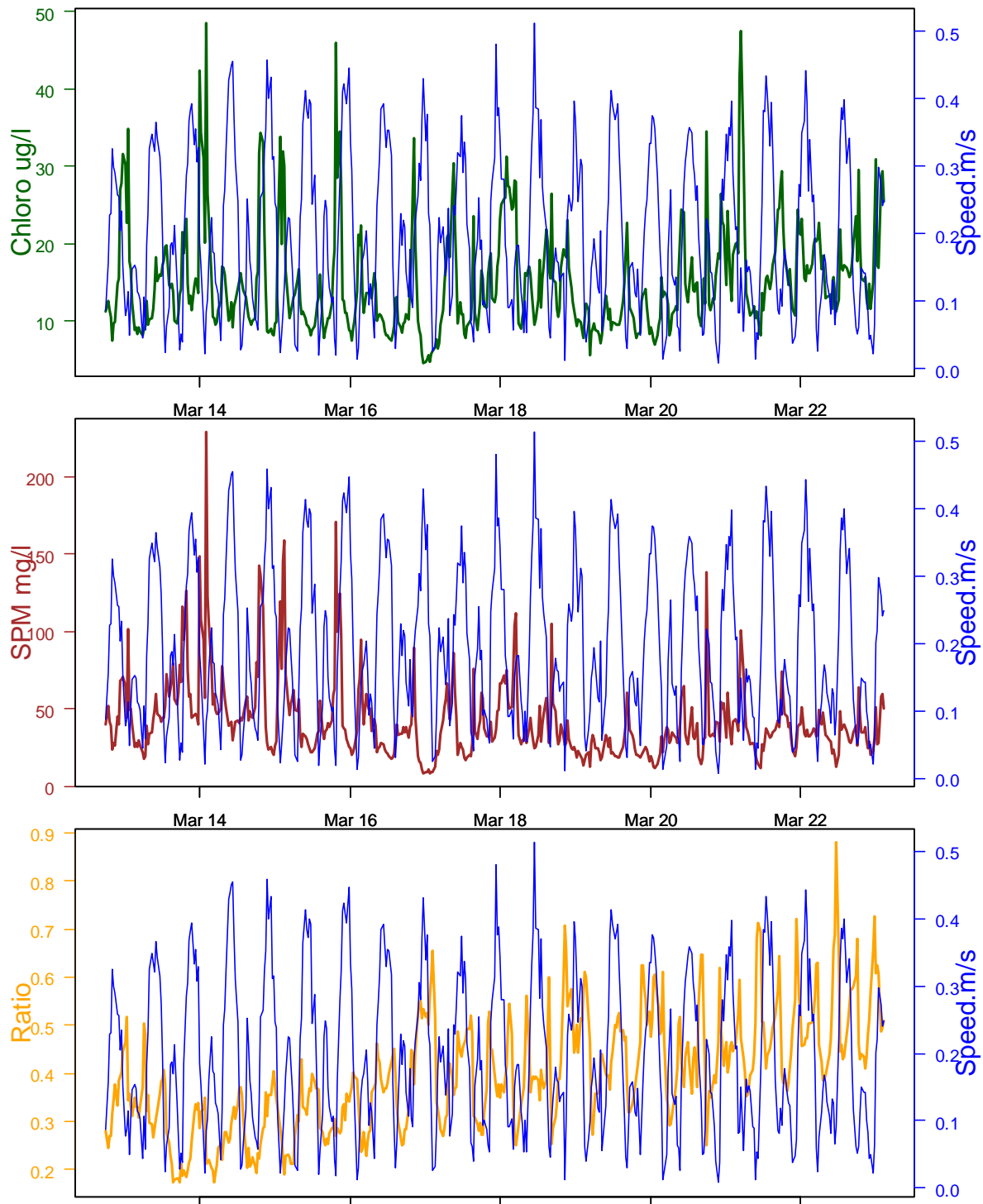


Figure 22. Timeseries of Chlorophyll, SPM and the Ratio (Chl-a/SPM) together with the measured current speed (150cm) in the spring period of 2010. The figure illustrates that both chlorophyll and total SPM show peak concentrations when current speeds are at minimum.

Valvometry

The *Ensis* used in the valvometry had a limited survival rate and in one of the first autumn period the hardware malfunctioned for unknown reasons. In the second spring period the measurements of chlorophyll and turbidity was not succesful. This effectively rendered us with one measurement series collected in spring and one in autumn for in depth analyses. For these two contrasting periods similar analyses were performed.

First the *Ensis* raw valve gape data were transformed to a relative valve opening (fraction from 100% open). These data sets were related to each other and in second instance related to environmental data which were collected at the same time. In the first deployment period only two animals survived and one died before the end of the deployment period. In the autumn deployment period (wk 41-wk 44) 6 animals survived.

Spring

The valve gape records of these three animals is depicted in Figure 23.

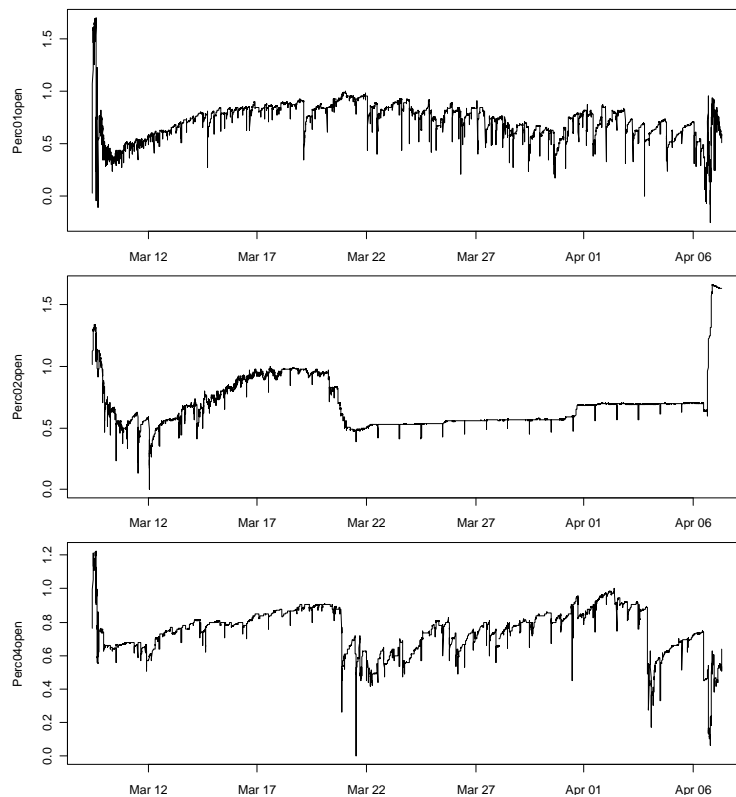


Figure 23. Valve gape over time. Valve gape is expressed as fraction open relative to maximum gape. Animal 02 (second panel) died before the end of the deployment.

All three individuals show temporally aligned valve gape response as illustrated when plotted against each other (Figure 24). The temporal alignment of the response differs over the study period. The graph (Figure 25) of the running correlation suggest that the similarity in valve response varies over time.

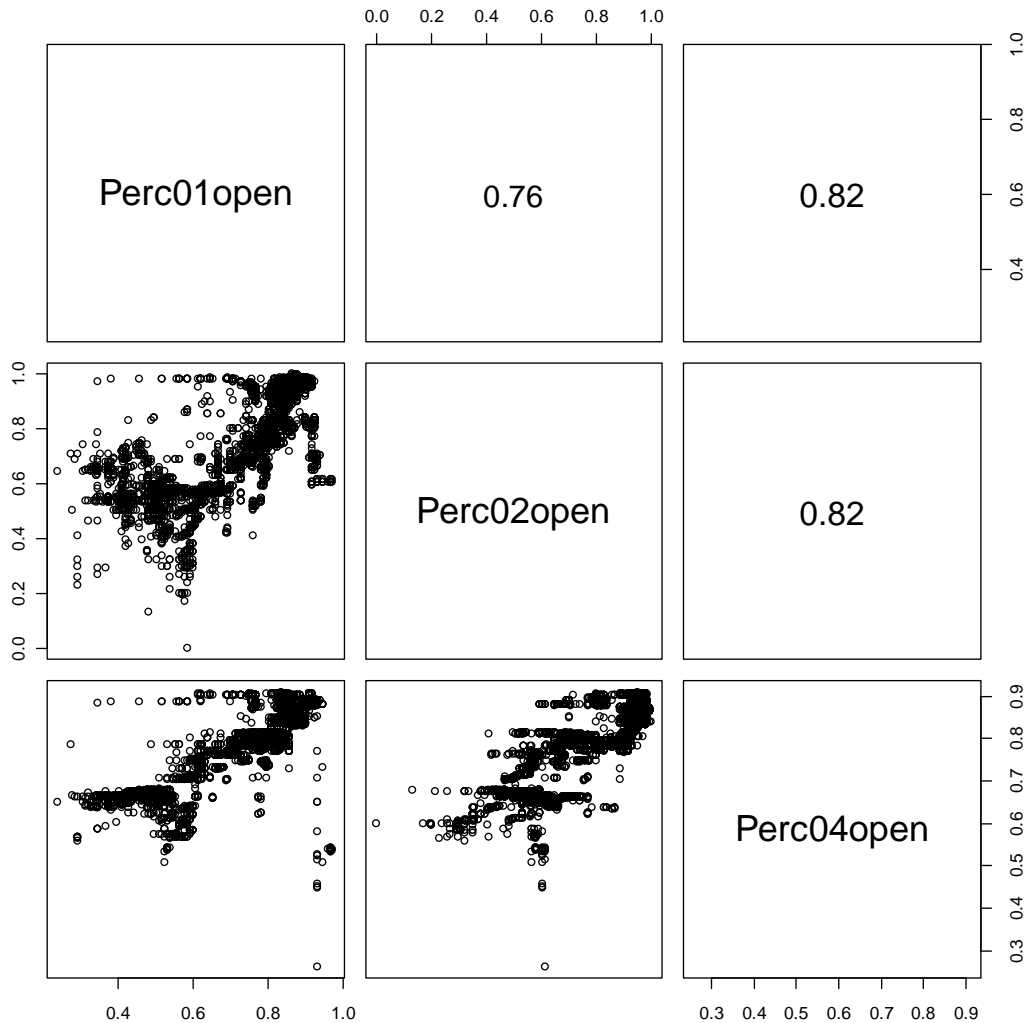


Figure 24. Plotting the raw valve gape fraction against each other for the longest period over which all three animals were alive (March 9th-March20th). The positive trend among the specimens show that there is a high degree of temporal similarity as what is given with the correlation coefficient in the upper panels.

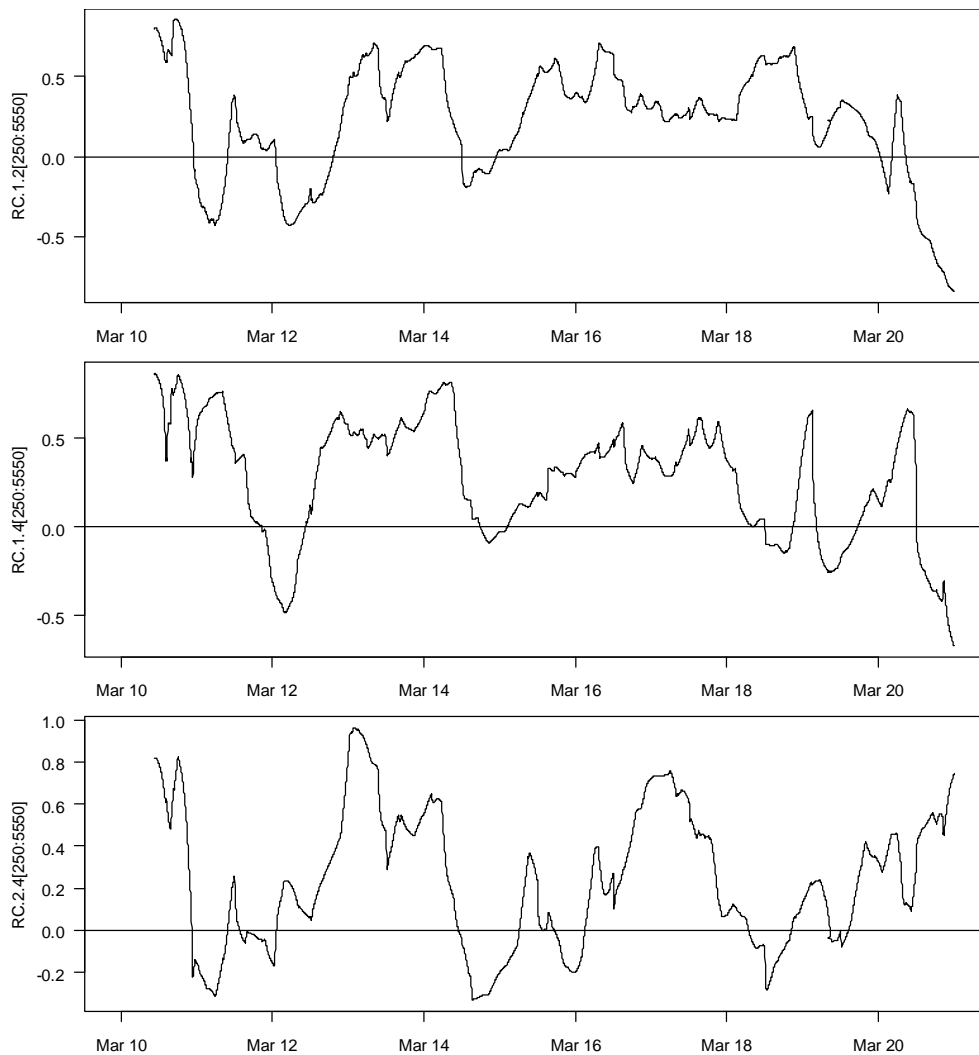


Figure 25. Height of a running correlation (1 day=480 measurements) for the period between March 9 and March 21st. The figure demonstrates the high correlation and temporal alignment of the valve response between the individuals used in the valve gape monitor.

Because these benthic bivalves rely for their food on material which sinks from the upper water column to the seafloor, the analyses to find an explanation for the variation in valve gape focused on its relation with chlorophyll and SPM measured in the near bottom waterlayer. In Figure 26 the max valve gape per 50 mg bins suspended sediment illustrates that with increasing sediment load, valve gape decreases. The top panel gives the linear regression over the maximum gape values for each of the 7 concentration bins. With the exception of specimen 2 (Perc02open) all show a decrease.

The lower panel gives the full dataset and the 0.90 fitted quantile regression lines. Figure 27 illustrates the relationship between valve gape and chlorophyll concentration as well as the ratio between chlorophyll and mud. Especially latter plots (Valve gape X ratio) suggest that the maximum valve gape of *Ensis* increases with

increasing ratios. Similar relationship is absent in the autumn series of measurements. This difference most likely illustrates the qualitative difference in material as illustrated by Figure 19

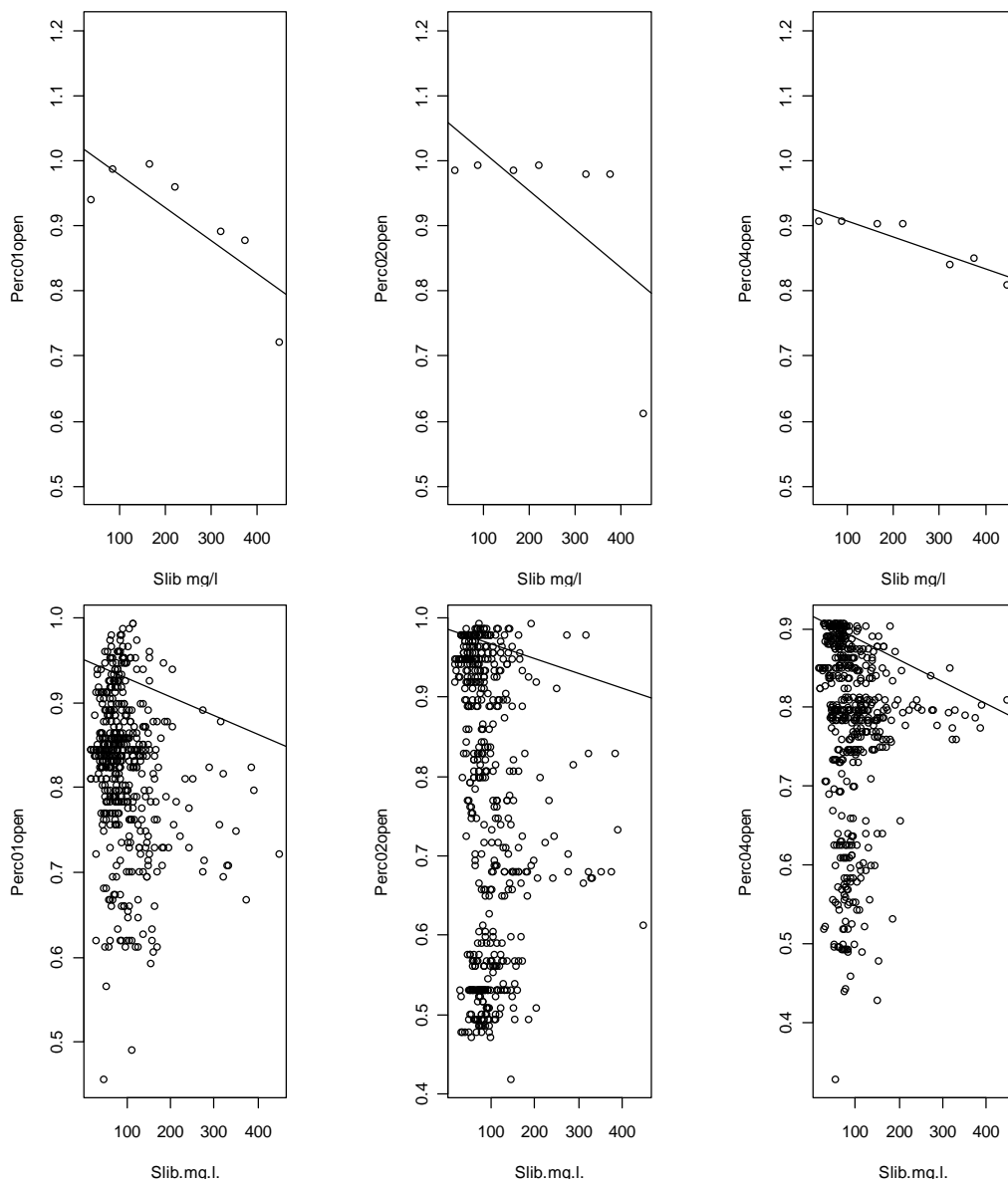


Figure 26. Plot of maximum valve gape for distinct maximum SPM (Slib.mg.l) concentrations determined for 50 mg bins (upper row of graphs). The lower row of graphs gives the complete dataset together with the fitted .90 quantile regression line between both variables. Illustrating the negative effect of high mud (Slib mg/l) concentrations on valve gape.

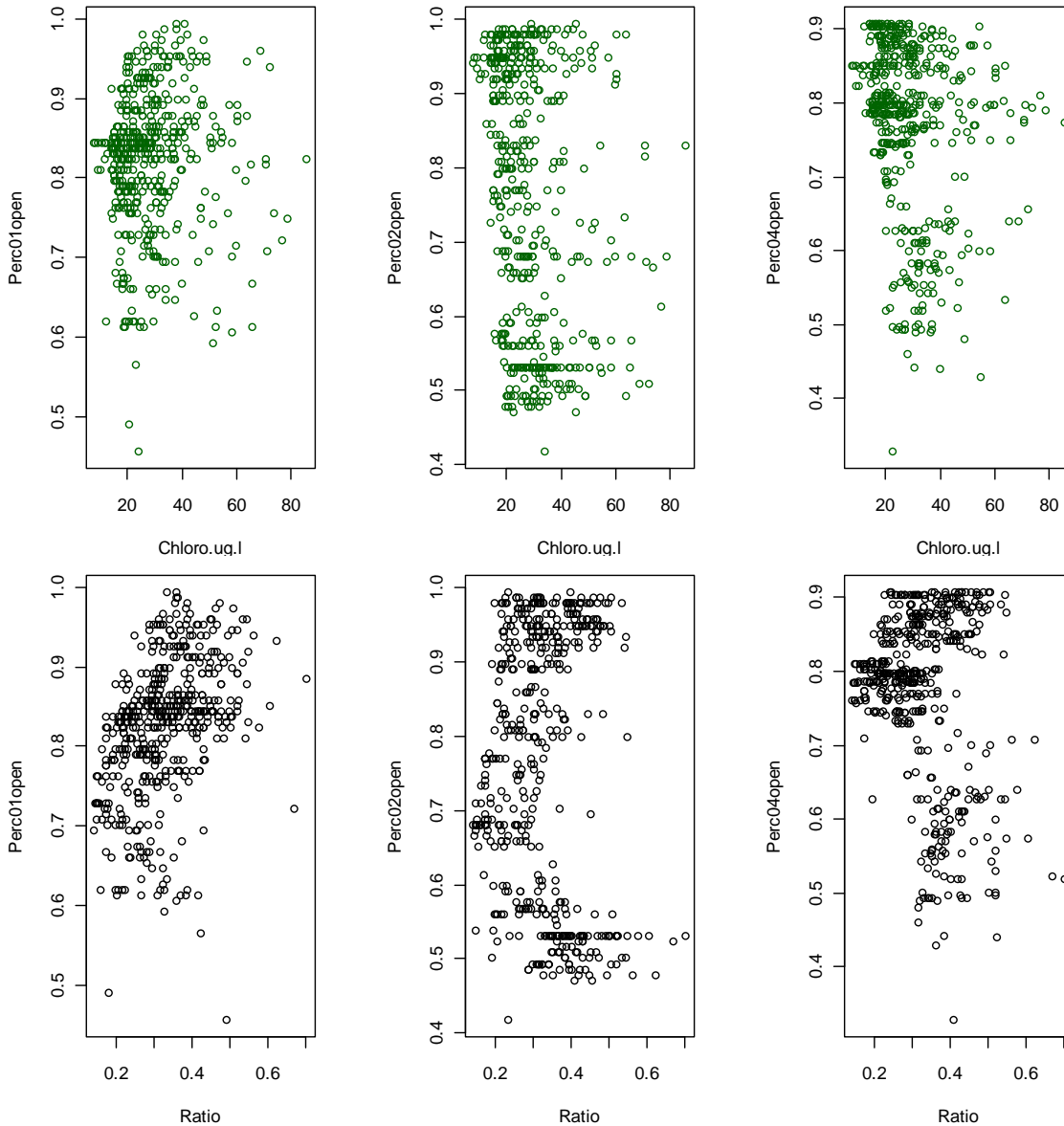


Figure 27. Plot of maximum valve gape for distinct maximum chlorophyll concentrations (upper panels) and Chlorophyll to Silt ratios (lower panels) in spring. Maximum valve gape has the tendency to increase with increasing chlorophyll to mud ratios.

Autumn

The autumn deployment yielded more valve gape records than the spring deployment. The same patterns emerge. The different individuals to a large extent show similar temporal variation in their record. A maximum correlation of .88 was found. Close inspection of shows that especially animal 3 behaves differently and has low correlations with all other specimens (Figure 28; Figure 29).

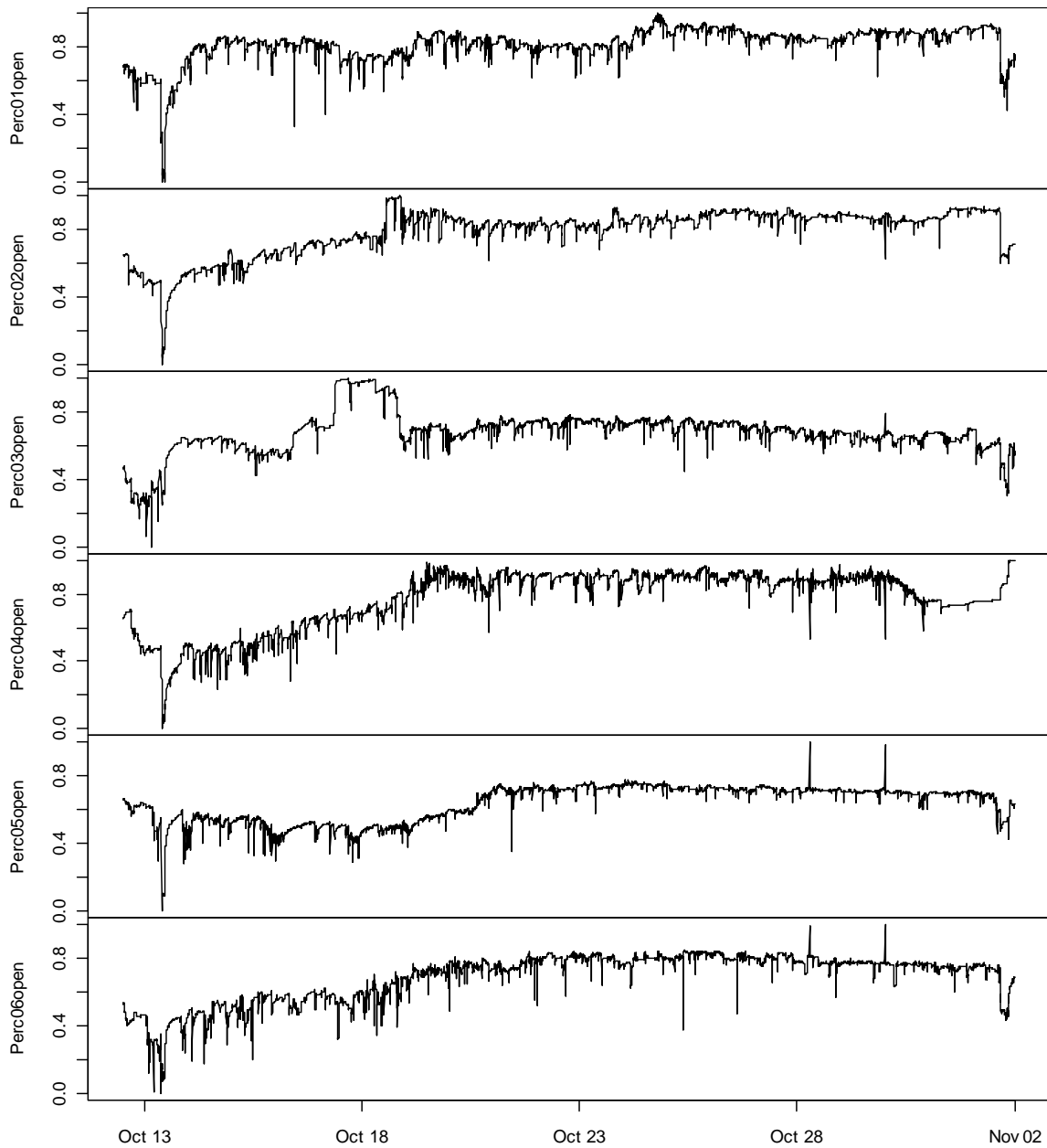


Figure 28. Ensis Valve gape response in autumn 2010. Six animals yielded good records of their valve gape.

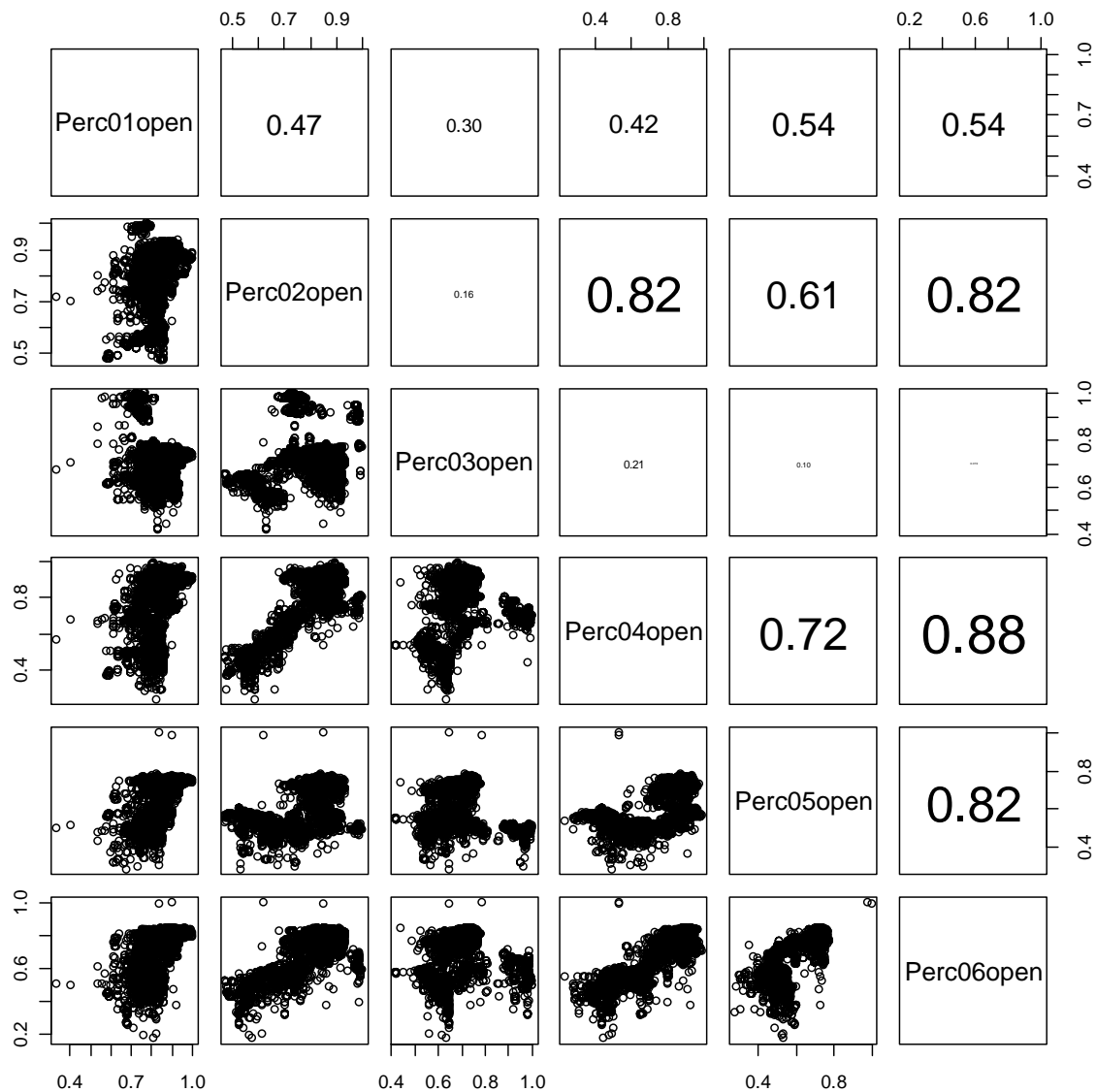


Figure 29. Pairs plot illustrating the similarity in valve gape response between 6 different individuals for the autumn measurement period between week 41 and week 44. top right panels give correlation coefficients of the combination of animals given on the diagonal. Animal 3 (Perc03open) has the weakest relationship with the other specimens.

From the above records max valve gape for 100 mg bins of suspended mud were extracted and related to the average mud concentration in this bin. The result shows that most individuals show a strong decrease in valve gape over the concentration range between about 300 and 1000 mg/l. This again suggests that Valve gape is negatively influenced by high concentrations of suspended mud (Figure 30).

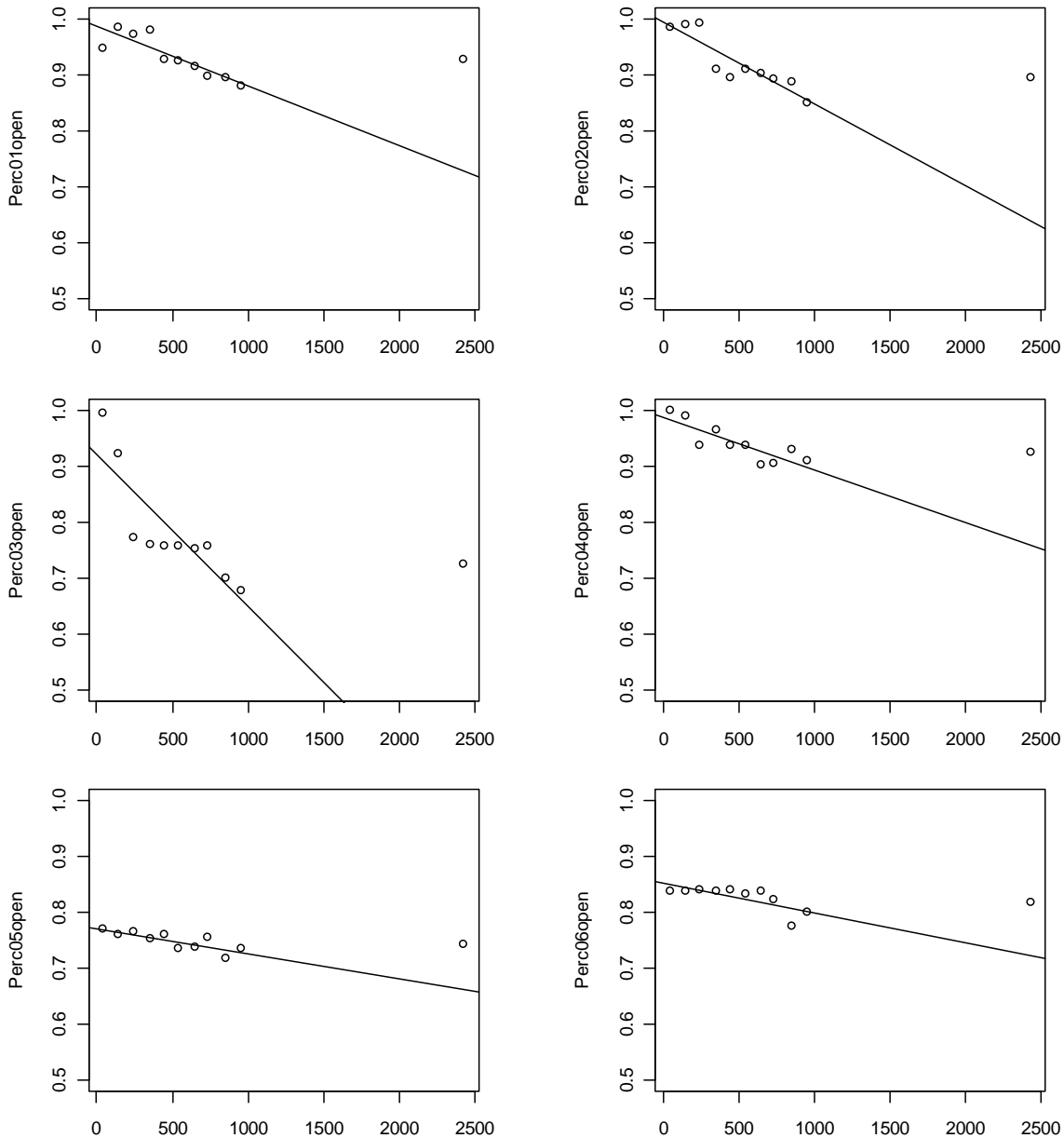


Figure 30. Relation between Valve gape (Y-axis) and mud concentration (X-axis). all specimens show an inverse relationship, i.e. with increasing mud concentrations they limit the valve gape.

Valve gape of these six autumn animals has also been plotted against the ratio between chlorophyll and mud (Figure 31). While in the spring deployment a positive tendency between both variables emerged, such relationship was absent in data set collected in autumn. Most likely this has to do with the seasonal difference in qualitative characteristics of the suspended material as illustrated in Figure 19.

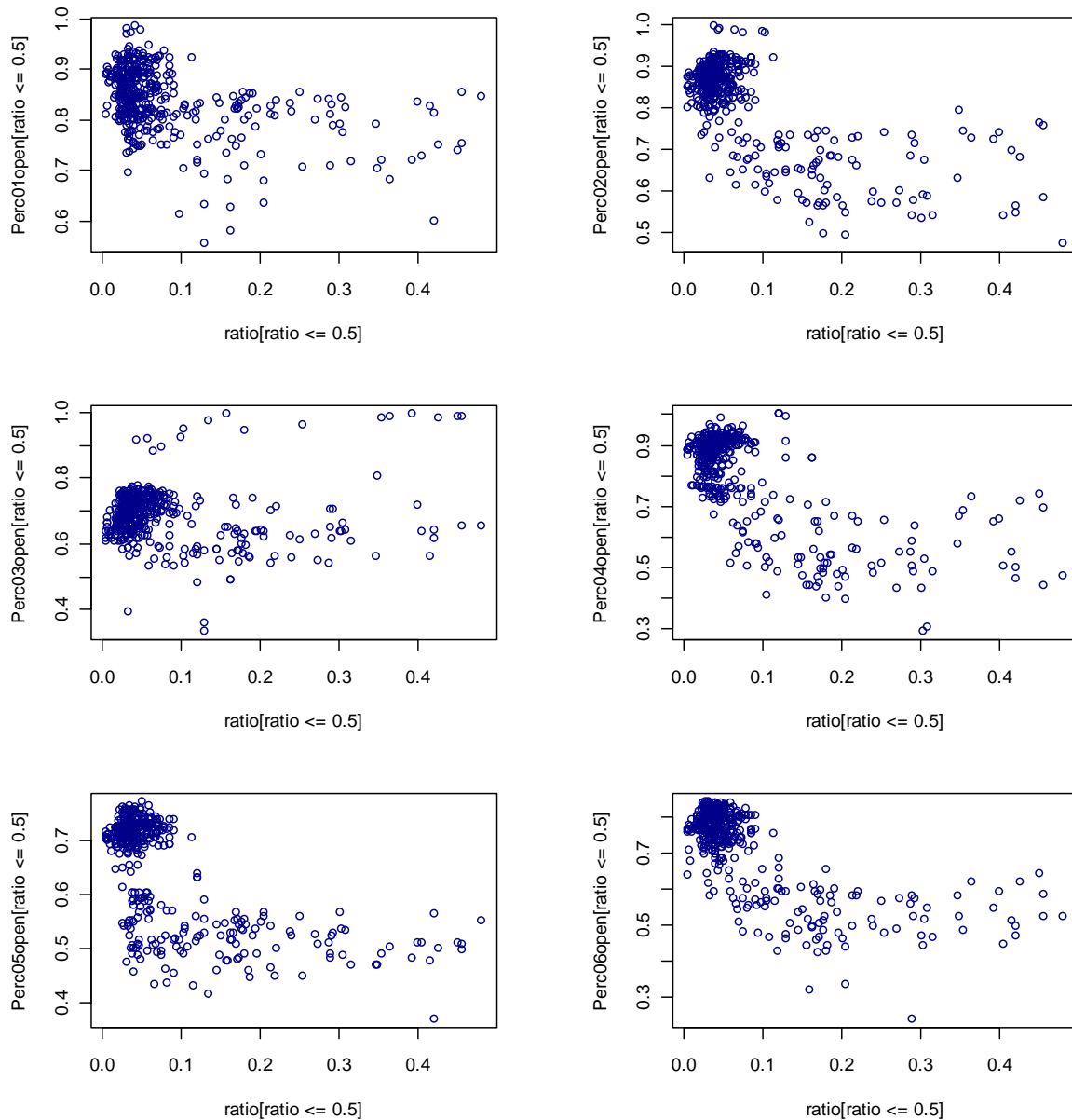


Figure 31. Relation between valve gape (Y-axis) and ratio of Chlorophyll to mud exclusively for the range of the ratio up to 0.5. This to make it comparable to figure 23.

Harbour experiment

Parallel to the spring deployment off the coast of Egmond, a similar experimental set up was made in the NIOZ harbour. 8 Ensis were equipped with sensors and local turbidity, chlorophyll and temperature were measured during the time of deployment. An overview of these parameters is given in Figure 32.

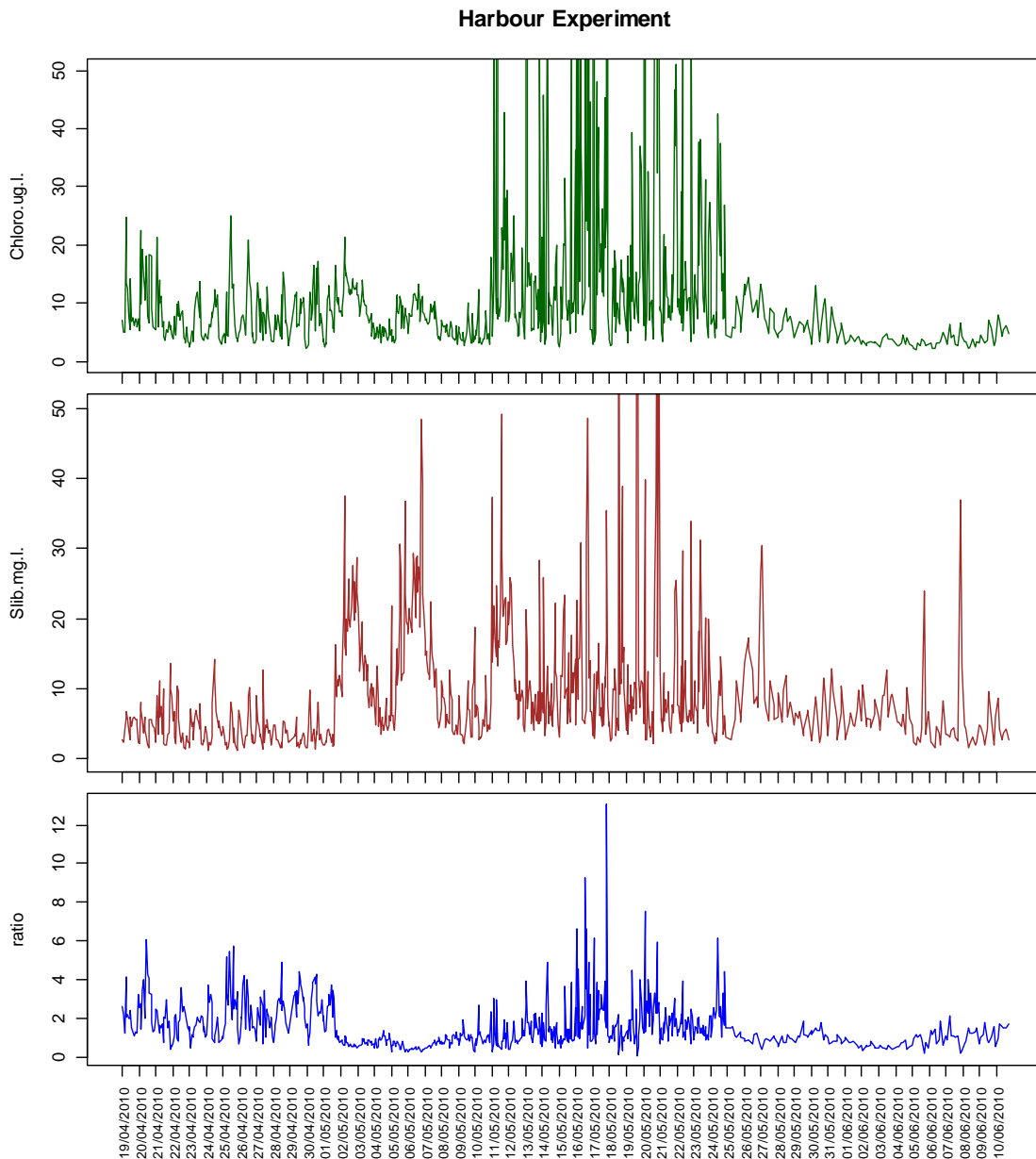
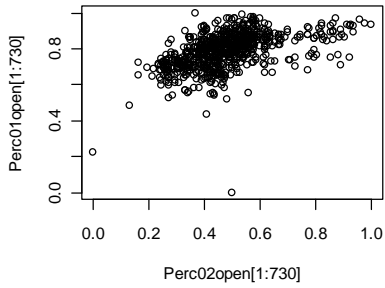


Figure 32. Chlorophyll and Silt concentrations in the harbour experiment between mid april and early June 2010.

In this experimental setup *Ensis* mortality was even higher than in the setup used on the lander. Despite repeated replacement of *Ensis*, only two valve gape records of sufficient length could be collected (Figure 33). Like the records obtained from the lander deployments both were highly correlated. Plotting the valve gape against the Chlorophyll and mud concentration as well as to the ratio suggests similar type of relationships as detected in the *Ensis* deployed at the lander off Egmond. The relationship between valve gape and mud (Figure 34) is less clear probably due to the relatively small range of mud concentrations. The graph showing relationship between

gape and on the other hand seems to be more distinct, but opposite to what could be expected for spring and what has been found off shore Egmond.



harbour experiment

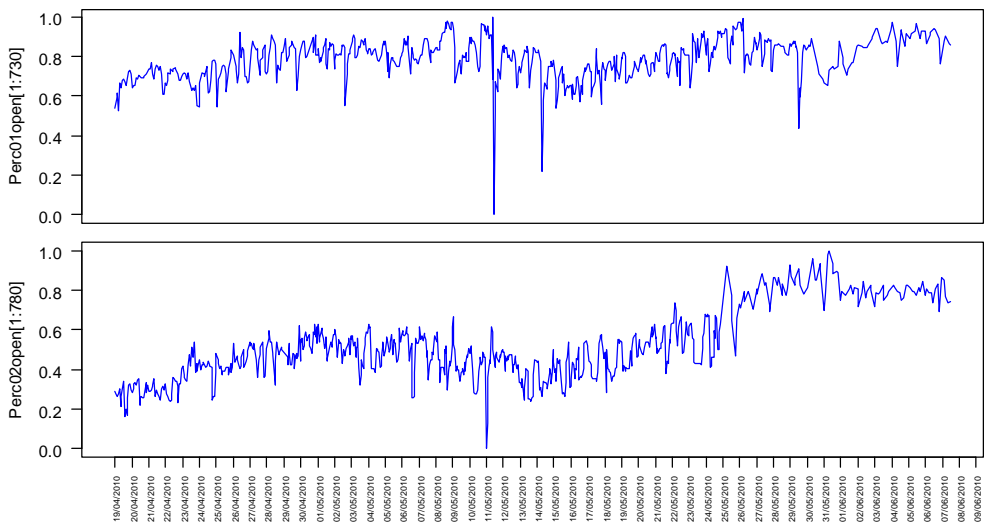


Figure 33. Two long valve gape records obtained from the harbour experiment in 2010. Correlation between both records is 0.82.

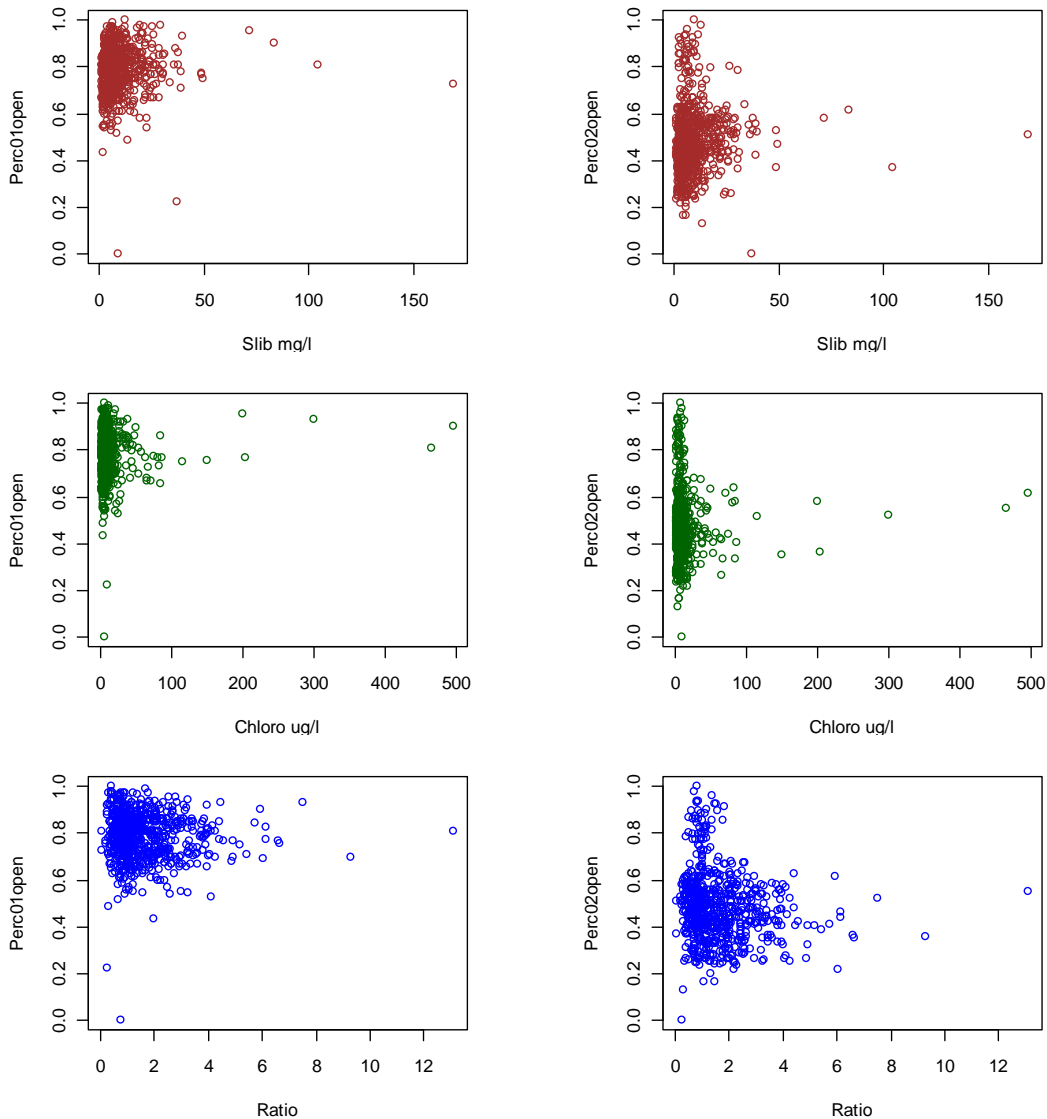


Figure 34. Valve gape response to Slib Concentration, Chlorophyll concentration. The range of concentrations is less than those encountered in the North Sea lander Deployments. Ratios are much higher, due to the relatively low mud concentrations, compared to normal bloom chlorophyll concentrations.

The second part of the "harbour" experiment aimed at the determination of shell and tissue growth and aimed at the use of these measurements to link it to the recorded valve gape. Hereto we started with 112 living specimens which were placed individually in tubes. All individuals were measured at the start of the experiment. For a control group from the same collection AFDW at the start of the experiment was determined. It was meant to monthly withdraw 10 random individuals and determine their shell and AFDW growth relative to the start length and estimated start weight. Due to high mortality this part of the experiment failed completely. Thus besides the

sparse valve gape records, no data on tissue growth and shell growth could be obtained.

DISCUSSION & SYNTHESSES.

For the off shore Egmond location two datasets of valve gape response and environmental variables could be collected. These data on valve gape and on environmental conditions have been pooled into one dataset. In the first dataset (collected in spring) a small change in temperature over time is apparent. Valve gape over this temperature range shows a strong positive relation. The valve gape data for the autumn period did not show any temperature effect (Figure 35). The presence of an underlying temperature \times valve gape relationship could imply that the observed negative trend of valve gape to the concentration of slib is the result of this covariate.

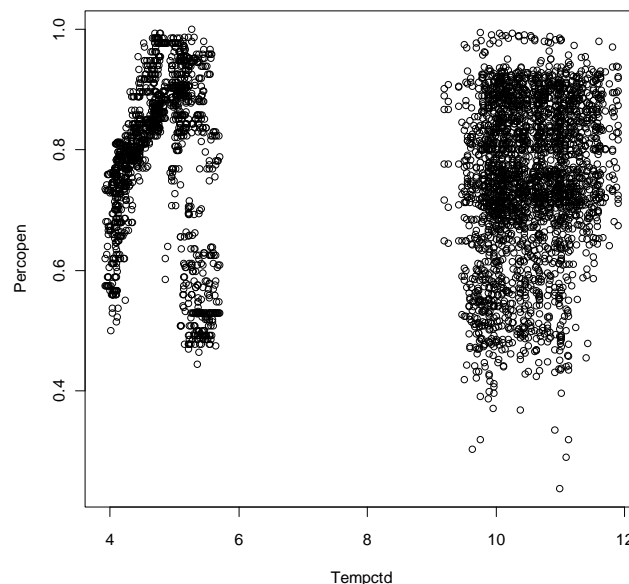


Figure 35. Valve gape times Temperature. In the spring period with temperatures starting at 4°C a rapid increase in valve gape is visible. In Autumn at temperatures between 9 and 12° C no trend is visible.

Therefore the data collected in spring was reanalysed again for an effect of mud concentration on valve gape after removal of the temperature effect from the valve gape data. This was done by working with the residual valve gape after regressing valve gape against temperature. This analyses showed that also in the residual of valve gape the maximum values had an inverse relationship to mud concentration (Figure 36), as shown in the analyses for the animal specific responses given earlier.

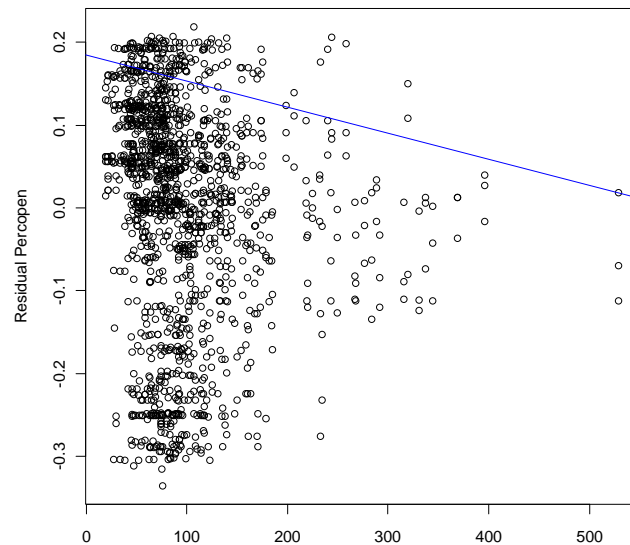


Figure 36. Residual valve gape after removal of the temperature effect as being dependent on mud concentration (mg/l). The fitted line is the .90 quantile regression. The figure suggests that also here maximum gape decreases with increasing mud concentrations.

The strong valve gape response to temperature over a very limited temperature in spring might suggest that there is a (not measured) covariate strongly influencing the behaviour of *Ensis* or alternatively that the water temperature of around 5°C (as prevalent in that period) is the minimum temperature below which the animals are inactive. Data which supports this hypothesis comes from the work of Cardoso et al, 2013. Their growth rate data, based on stable isotopes, suggest that ~6 °C is the lowest temperature at which shell growth occurs. Most shell growth was observed at recalculated temperatures of 14 °C or higher. This suggests that 6°C is in the lower range at which *Ensis directus* is metabolically active.

The two distinct temperature ranges over which valve gape records were collected together with the different behaviour over these two temperature ranges makes a multivariate analyses of the entire data set complicated. Furthermore the effects of the various variables measured not necessarily have linear relationships. Therefore a generalized additive modelling was applied to the Egmond field data. For above reasons and uncertainties, in this analyses the effect of temperature was neglected. In first instance the entire data range was used, i.e. all matching valve gape and environmental records. This led to minimal though still significant model estimations (Figure 37.)

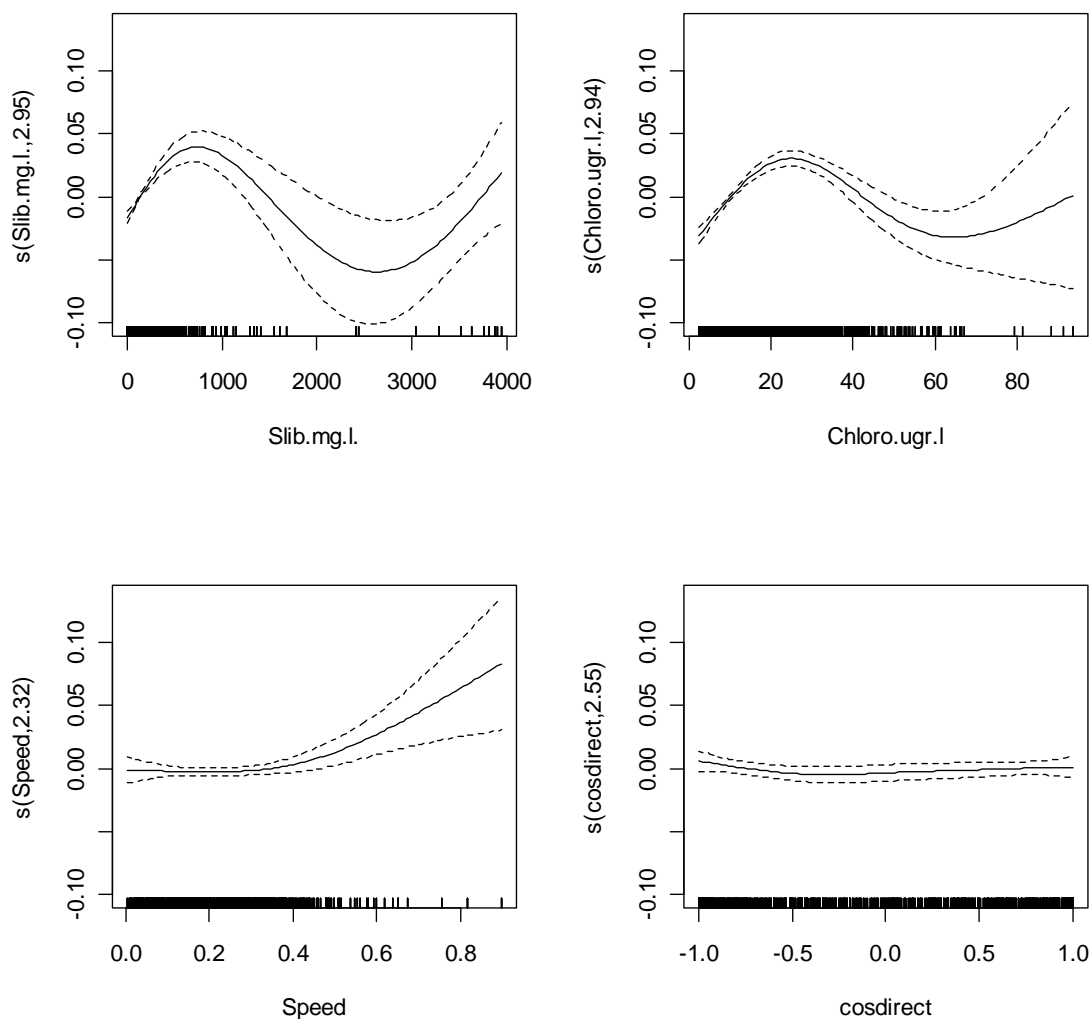


Figure 37. GAM smoother functions ($s(\cdot)$) describing the behaviour of valve gape as a smoother function of SPM, Chlorophyll, Speed or direction. Silt and chlorophyll concentrations are those measured at 30 cm above the seafloor, the approximate height at which the *Ensis* were deployed. Dotted lines indicate 95% certainty around the estimated smoother. The quantity along the y-axis gives the change in valve gape (%) over the range of SPM, Chlorophyll, Current speed and current direction. Data density is given as vertical ticks along the x-axis.

Figure 37 depicts the smoother functions describing the change in valve gape being dependent on the variable given in each of the panels ($s(\text{Slib.mg/l})$, $s(\text{Chloro.ugr/l})$, $s(\text{Speed})$; $s(\text{cosdirect})$). Current direction (expressed as the cosine of the current direction) has no effect on valve gape, i.e. the magnitude of the smoother stays around zero. Over the normal range of current speed measurements, up to 0.5 m/s no effect of current speed is visible either. At higher currents there is an increase but the error around the estimate increases considerably, due to the limited number of measurements. This observed tendency may suggest that under certain conditions, for instance in autumn, resuspension caused by high current speeds makes food

particles available in an otherwise food poor period, leading to a slightly higher valve gape.

Variables which more directly influence valve gape are the chlorophyll concentration and mud concentration (Figure 37). Here again the low number of measurements in the higher concentration levels contributes to a rather large uncertainty. The smoother functions illustrate that the valve gape responds to the concentration of mud and chlorophyll like an optimum curve. The graphs suggest that at increasing mud concentrations the valve gape initially increases, but if concentrations continue to increase valve gape does not change anymore and in the end even decreases. In some of the individual data sets this increasing valve gape at low concentrations is visible. The same holds for the chlorophyll concentration. Up to about 20 ug chl-a / liter there is a steady increase in valve gape but further increases in the concentration lead to a decrease in valve gape. It should however be noted that the data density in the higher concentrations ranges is much lower than in the lower range. Hence the uncertainty around the fitted smoother function dramatically increases.

Limitation of the dataset to mud concentrations lower than 750 mg /l yields similar response in relation to all used variables but the fitted models are to a lesser degree determined by the sparse data at the high end of the data range. Although explained deviance is low the fitted models appear to be significant, also because of the high number of measurements used to fit the model (~4000 datapairs).

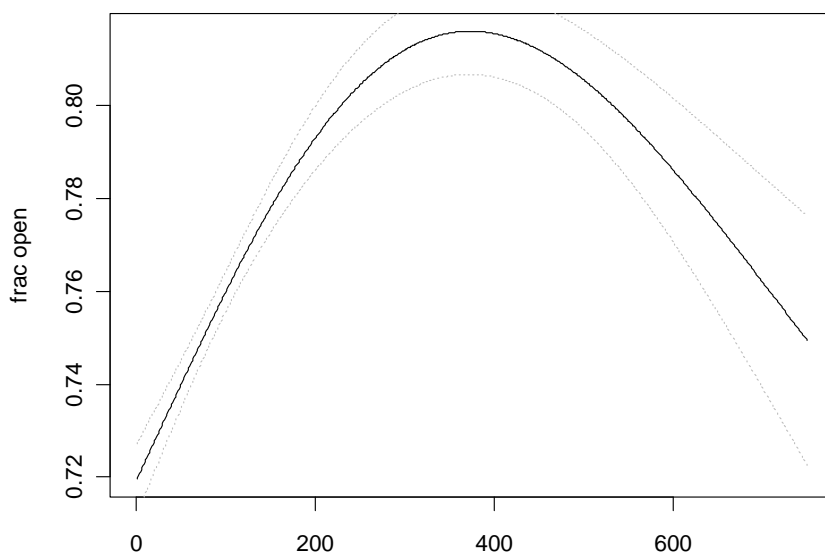


Figure 38. Fitted Valve gape (frac open) over the measured mud concentration (x-axis) up to 750 mg/l.

And idealized relationship between mud concentration and valve gape response, based on the gam model is given in Figure 38. This figure shows the increase in valve gape at concentrations lower than about 400 mg/l. This is much higher when compared to results obtained in lab studies in which 200 mg kaolinite/l reduced clearance rate in *Ensis* significantly. But both results suggest that increasing mud concentrations lead to a decrease in valve gape or clearance. The significance of valve gape in relation to filtration rates and feeding is however not yet explored. A recently published experimental study Kamermans et al (2013) observed that filtration rate at mud concentrations of 300 mg/l are reduced but that this did not lead to reduced growth rates. Lowering the amounts of chlorophyll however did. Hence Kamermans et al concluded that *E. directus* is more sensitive to a reduction in algal concentration than to an increase in mud concentration.

The results presented in this study showed that both the concentration of SPM and of Chlorophyll have a similar (optimum) response curve. The response curve between valve gape and SPM concentration in the field support the findings by Kamermans et al. Only at concentrations higher than 300-400 mg/l result in a reduced valve gape and most likely a lowered filtration rate.

CONCLUSIONS

In the research area the average *Ensis* density is 265 individuals / m². There are three cohorts in the area present. They have approximate sizes of 50, 80 and 120 mm. Highest densities appear to be found close to the coast. Further offshore densities decrease, but average size is larger.

Shell growth takes place between the end of April and mid September. Condition index probably peaks in May and June.

The data collected in the near coastal environment of Egmond shows a marked seasonal variation in the ratio between Chlorophyll and Silt. There are also marked tidal effects on the quality, quantity and distribution of Silt and Chlorophyll above the bottom. Highest concentrations are found closest to the seafloor and strongly dependent on tidal currents. During the measurement periods in autumn 2010 two events have been observed at which concentrations of mud surpass 2500 mg/L. The associated increase in the chlorophyll concentrations suggest that organic material is

either attached to this sedimentary material or that chlorophyll rich particles respond in a similar way as inorganic particles. In any case this resuspended chlorophyll rich material can potentially act as food source for filter feeders.

The analyses of obtained field data suggest that valve gape decreases when mud concentrations surpass concentrations of about 400 mg/l. The consequence of this decrease on assimilation and growth remains unknown.

REFERENCES

Alphen van, J.S.L.J. (1990) A mud balance for the Belgian-Dutch coastal waters between 1969 and 1986. *Neth. J. Sea Research* 25, 19-30.

Archambault M.-C, Bricelj V.M., Grant J., Anderson D.M., 2004. Effects of suspended and sedimented clays on juvenile hard clams, *Mercenaria mercenaria*, within the context of harmful algal bloom mitigation. *Marine Biology* 144: 553-565.

Cardoso J. F. M. F., G. Nieuwland¹, R. Witbaard¹, H. W. van der Veer¹, and J. P. Machado. Growth increment periodicity in the shell of the razor clam *Ensis directus* using stable isotopes as a method to validate age. *Biogeosciences*, 10, 4741–4750, 2013

Ellerbroek, G., M.J.C. Rozemeijer, J.M. de Kok, J. de Ronde, 2008. Monitoring and Evaluation Programme Sand mining RWS LaMER, part B5 of the evaluation programme Sand mining. Ministerie van verkeer en waterstaat, Noord holland.

Goudswaard, P.C.; Kesteloo, J.J.; Perdon, K.J.; Jansen, J.M., 2008. Mesheften (*Ensis directus*), halfgeknotte strandschelpen (*Spisula subtruncata*), kokkels (*Cerastoderma edule*) en otterschelpen (*Lutraria lutraria*) in de Nederlandse kustwateren in 2008. Yerseke : IMARES, (Rapport / IMARES C069/08)

Goudswaard P.C., K.J. Perdon, J.Jol, J.J. Kesteloo, C. van Zweeden & K. Troost, 2011. Schelpdieren in de Nederlandse kustwateren Bestandsopname 2011. Imares rapport c094/11 78pp.

Kamermans, P., E. Brummelhuis, M. Dedert, 2013. Effect of algae- and silt concentration on clearance- and growth rate of the razor clam *Ensis directus*, Conrad. *J. Exp. Mar. Biol. Ecol*, 446:102-109.

Kok, de J. M., 2004. Slibtransport langs de Nederlandse kust. Bronnen, fluxen en concentraties. Rapport RIKZ/OS/2004.148w: 31pp.

Vries, S. de, & R.L. Koomans, 2010. Monitoring van het slibgehalte in de toplaag van de zeebodem. Medusa, Groningen, 36pp.

Witbaard, R. & P. Kamermans, 2011. De bruikbaarheid van de klepstandmonitor op *Ensis directus* ten behoeve van de monitoring van aan zandwinning gerelateerde effecten. NIOZ rapport 2009-10, 44 pp